Seasonal variation in remotely-sensed phytoplankton size structure around Southern Africa.

T. Lamont[1,2], R. J. W. Brewin[3,4], R. G. Barlow[5,2].

[1] Oceans & Coasts Research, Department of Environmental Affairs, Private Bag X4390, Cape Town, 8000, South Africa

[2] Marine Research Institute and Department of Oceanography, University of Cape Town, Private Bag X3, Rondebosch, 7701, South Africa

[3] Plymouth Marine Laboratory (PML), Prospect Place, The Hoe, Plymouth PL1 3DH, UK

[4] National Centre for Earth Observation, PML, Prospect Place, The Hoe, Plymouth PL1 3DH, UK

[5] Bayworld Centre for Research & Education, 5 Riesling Road, Constantia, 7806, Cape Town, South Africa

Corresponding author email: tarron.lamont@gmail.com

Abstract

The three-component model of Brewin et al. (2010) computes fractional contributions of three phytoplankton size classes (micro- (> 20 μm), nano- (2-20 μm), picophytoplankton (< 2 μm)) to the overall chlorophyll *a* concentration (Chla). Using *in situ* pigment data, model coefficients were adjusted for application to the southern African marine region. The refined model was applied to seasonal and monthly climatologies of MODIS Aqua Chla around Southern Africa. Chla > 1 mg m^{-3} was limited to shelf regions along the coasts of Southern Africa and Madagascar, while values < 0.1 mg^{-3} were found over most of the open ocean between the equator and 38 °S during austral summer and autumn. In winter and spring, low values (< 0.1 mg m^{-3}) were restricted to smaller regions within subtropical gyres, while values up to 0.7 mg m^{-3} extended over a much greater area of the open ocean. Shelf regions in the northern (NB) and southern Benguela (SB), Agulhas Bank (AB), Agulhas region (AR), and Mozambique Channel (MC) all showed similar seasonal cycles of size structure. On average, micro-phytoplankton comprised > 50 % of the total Chla in these regions with little change throughout the year. The AR shelf differed, with picophytoplankton dominating in summer, and micro- and nanophytoplankton the rest of the year. In the open ocean domains of the NB, SB, and AB regions, nanophytoplankton dominated for most of the year, with picophytoplankton being more prevalent during summer and autumn. In contrast, in the AR open ocean, nanophytoplankton were dominant only during winter and early spring, whereas picophytoplankton dominated throughout the year in the MC open ocean. The refined model characterised previously unknown spatial and temporal changes in size structure in various ecosystems around Southern Africa.

Keywords: Phytoplankton, biomass, size structure, Benguela Upwelling System, Agulhas Current System, sub-Antarctic zone

1. Introduction

Phytoplankton play a critical role in a number of key marine processes, including the modulation of food webs, CO_2 exchanges, and the cycling of carbon and other nutrients such as nitrate, phosphate, and silicate. The size distribution of phytoplankton has a strong influence on community structure, physiology, metabolism, and the trophic organisation of the pelagic ecosystem (Chisholm, 1992). Partitioning phytoplankton communities according to size provides a more detailed and integrative means of investigating phytoplankton structure and function in relation to key physical processes and biogeochemical cycles (IOCCG, 2014). Communities dominated by large-sized phytoplankton have the potential to export organic, through a short food chain, to the seabed or transfer it to upper trophic levels and to neighbouring regions, while communities predominated by small-sized phytoplankton are mainly characterised by complex microbial food webs that favour recycling of organic matter within the euphotic zone (Cermeño et al., 2006). Although large-sized phytoplankton can sustain higher rates of photosynthesis (Cermeño et al., 2006), small-sized phytoplankton are an important fraction (35-60 %) of the total biomass and may account for over 50 % of daily primary production in oligotrophic regions and 25-30 % in more productive coastal regions (Platt et al., 1983; Tremblay and Legendre, 1994; Marañón et al., 2001).

The marine region around Southern Africa hosts a complex interplay between a number of major oceanic systems including the Benguela upwelling system, the greater Agulhas Current system, and the Southern Ocean, and plays a key role in the global ocean circulation and biogeochemical cycling (Hutchings et al., 2009; Lutjeharms, 2006). On the west and south coasts of Southern Africa, the Benguela upwelling system and the Agulhas Bank have ecological and economic significance for driving a very productive ecosystem which supports

a complex trophic structure and a multitude of commercially harvested resources (Hutchings et al., 2009; Verheye et al., 2016). Most of the primary production in this ecosystem can be attributed to microphytoplankton dominated communities, but nanophytoplankton dominated communities are also known to be important due to their larger spatial extent (Hirata et al., 2009).

Located on the east and south coasts of Southern Africa, the Agulhas Current system feeds the upper limb of the Atlantic meridional overturning circulation through the flow of warm, saline surface waters from the Indian Ocean to the Atlantic Ocean (Lutjeharms, 2006). The Agulhas ecosystem and Mozambique Channel are characterised as oligotrophic, where mainly nano- and picophytoplankton dominate in the surface layers further offshore, with microphytoplankton being more important in the shelf regions (Barlow et al., 2010; Sá et al., 2013). Located south of the African continent, the Southern Ocean plays a critical role in regulating the global organic carbon flux and modulates nutrient supply to thermocline waters, which in turn drives productivity in the lower latitudes (Sarmiento et al., 2004; Schlitzer, 2002). The Southern Ocean is unique in that it has high nutrient concentrations and low phytoplankton biomass, with high spatial and temporal variability (Thomalla et al., 2011a). These extremely different environments provide a good opportunity to investigate seasonal variations in phytoplankton biomass and size structure under varying environmental conditions.

With decreasing opportunities and continually rising costs associated with the collection of *in situ* data, research efforts globally have become more focussed on the use of satellite data and models to elucidate oceanographic processes and variability (IOCCG, 2014). In recent years, the use of satellite ocean-colour data has been extended to the derivation of phytoplankton

functional types and size classes, with the aim of improving our understanding of oceanic biogeochemical cycles. A number of different abundance-based, spectral-based, and ecological approaches to determine phytoplankton size classes (PSC) have been developed and implemented (Brewin et al., 2010; Hirata et al., 2009; Uitz et al., 2006, among others). Although Brewin et al. (2011) highlighted the need for continued and improved *in situ* data availability to further improve the estimation of satellite-derived PSCs, their initial comparison indicated that the various models performed with similar accuracy. While these models have been applied globally, there have been relatively few models tuned for regional applications, and none for around Southern Africa. One approach that has been successfully tuned to different regions is the three-component model of Brewin et al. (2010), including: the Atlantic Ocean (Brewin et al., 2010; Brewin et al., 2014); the eastern Atlantic Ocean (Brotas et al., 2013); the Indian Ocean (Brewin et al., 2012); the South China Sea (Lin et al., 2014); the Western Iberian coastline (Brito et al., 2015); the Mediterranean Sea (Sammartino et al., 2015); the Red Sea (Brewin et al., 2015a); as well as the global ocean (Brewin et al., 2015b; Ward, 2015). The primary goals of this study are to: (1) refine the parameterization of the Brewin et al. (2010) model for regional application to the marine environment around Southern Africa; (2) to use the model to identify the dominant size class; and (3) describe previously unknown seasonal and spatial variations in Chla and phytoplankton size structure in this region.

2. Data and Methods

2.1. Re-tuning of the Brewin et al. (2010) model

Brewin et al. (2010) developed an abundance-based PSC model to estimate the Chla concentrations of three phytoplankton size classes (micro- (> 20 μm), nano- (2-20 μm), and

picophytoplankton (< 2 μm)), as a function of the total Chla concentration (*C*). The model is based on two exponential functions (Sathyendranath et al., 2001), where the chlorophyll concentration of picophytoplankton (denoted C_p) and combined nano-picophytoplankton (denoted $C_{p,n}$) are computed as:

$$C_p = C_p^m\left[1 - exp\left(S_p C\right)\right], \quad (1)$$

and

$$C_{p,n} = C_{p,n}^m\left[1 - exp\left(S_{p,n} C\right)\right], \quad (2)$$

where the parameters $S_{p,n}$ and S_p determine the initial slope between size-fractionated chlorophyll and total chlorophyll (denoted C in the Eq. 1 and 2), and C_p^m and $C_{p,n}^m$ determine the asymptotic maximum values for the two size-classes. Once $C_{p,n}$ and C_p are obtained, nanophytoplankton chlorophyll (denoted C_n) and microphytoplankton chlorophyll (denoted C_m) can be computed as $C_n = C_{p,n} - C_p$ and $C_m = C - C_{p,n}$. The fractions of each size class (F_p, F_n and F_m) can then be computed by dividing the size-fractionated chlorophyll (C_p, C_n and C_m) by total chlorophyll (*C*).

The original global model was parameterized using coefficients determined from refined relationships between HPLC (High Performance Liquid Chromatography)-derived biomarker pigments and the total Chla (Uitz et al., 2006), and linking specific biomarker pigments to each size class following Uitz et al. (2006), with further refinements as proposed by Brewin et al. (2010) and Devred et al. (2011). Details of the development, parameterisation and application of the model are described in Brewin et al. (2015b). Application of the model to satellite data has been extensively validated with independent *in situ* data in a variety of marine environments (Brewin et al., 2010; Brewin et al., 2012; Brewin et al., 2015b; Lin et al., 2014).

Here, we regionally-tuned the global model using HPLC data collected in the Southern African marine region (Figure 1). This included data from: the BEAGLE cruise (November-December 2003; Barlow et al., 2007); the Atlantic Meridional Transect (AMT) cruises 6, 15, 16, and 17 (May 1998, October 2004, May 2005, November 2005; Brewin et al., 2010); the Agulhas ecosystem and Tanzania (November 2006, August-October 2007; Barlow et al., 2008; Barlow et al., 2011); the Mozambique Channel (November-December 2008, October-November 2009, April-May 2010; Barlow et al., 2014); Version 2.0 ALPHA of the NASA bio-Optical Algorithm Dataset (October 2002; Werdell and Bailey, 2005), following the removal of any AMT data so as to avoid duplication; and a cruise in the Atlantic sector of the Southern Ocean (February-March 2009; Gibberd et al., 2013). Only samples in the top 20 m of the water column were used (within the surface mixed-layer, rarely < 20 m, de Boyer Montégut et al., 2004), and where the difference between Chla and the total accessory pigments was less than 30 % of the total pigment concentration (Aiken et al., 2009; Brewin et al., 2015b). In total, 407 samples were available and Figure 2a shows the spatial distribution and number of samples for each dataset.

Following the methods described in Brewin et al. (2015b), size-fractionated chlorophyll (C_p, C_n and C_m) was estimated from the HPLC pigment data. The total chlorophyll concentration was estimated from the weight of seven diagnostic pigments (Uitz et al., 2006), and then the fractions of chlorophyll in each size class were estimated. The fraction of picophytoplankton chlorophyll (C_p) was computed using zeaxanthin, total chlorophyll *b*, and by allocating part of the 19'-hexanoyloxyfucoxanthin pigment to the picophytoplankton pool at total chlorophyll concentrations ≤ 0.08 mg m^{-3}. The nanophytoplankton chlorophyll fraction (C_n) was estimated using 19'-hexanoyloxyfucoxanthin, 19'-butanoyloxyfucoxanthin, alloxanthin,

and by apportioning some of the fucoxanthin pigment to the nanophytoplankton pool, using the method of Devred et al. (2011). The microphytoplankton chlorophyll fraction (C_m) was estimated using the remaining fucoxanthin (that was attributed to the micro size class) and peridinin as diagnostic pigments (Devred et al., 2011; Brewin et al., 2015b).

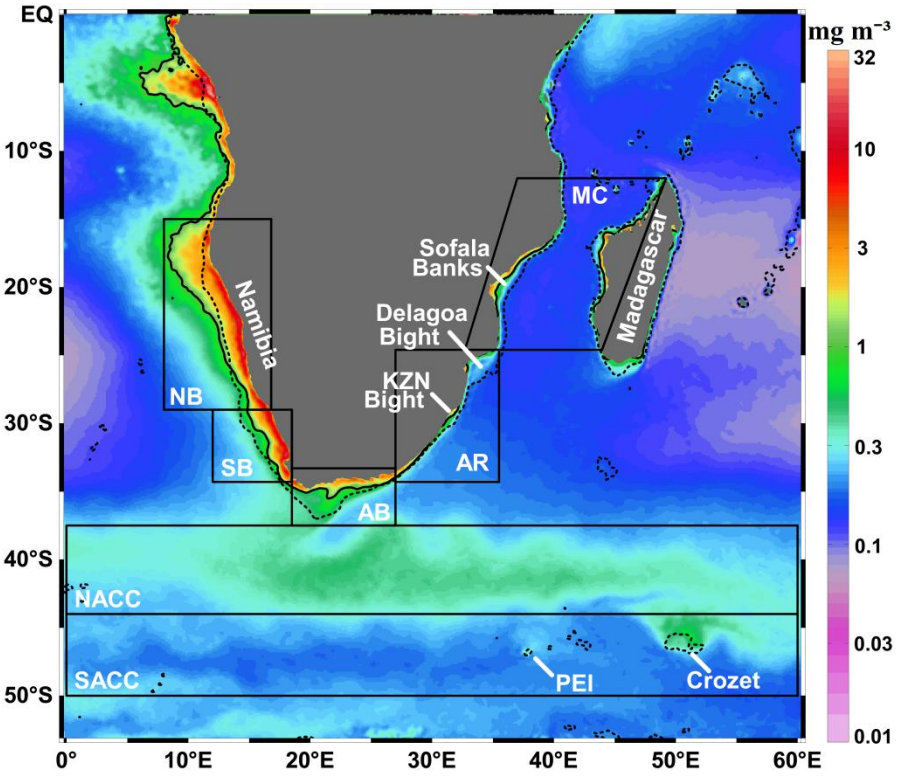

Figure 1: Long-term mean MODIS-Aqua chlorophyll *a* (mg m^{-3}) around Southern Africa with demarcated regions. (NB – Northern Benguela, SB – Southern Benguela, AB – Agulhas Bank, AR – Agulhas Region, MC – Mozambique Channel, NACC – Northern Antarctic Circumpolar Current region, SACC – Southern Antarctic Circumpolar Current region, PEI – Prince Edward Islands). Black solid contours indicate the 1 mg m^{-3} isoline, and the dotted black contours indicate the GEBCO 1000 m isobath (Becker et al., 2009).

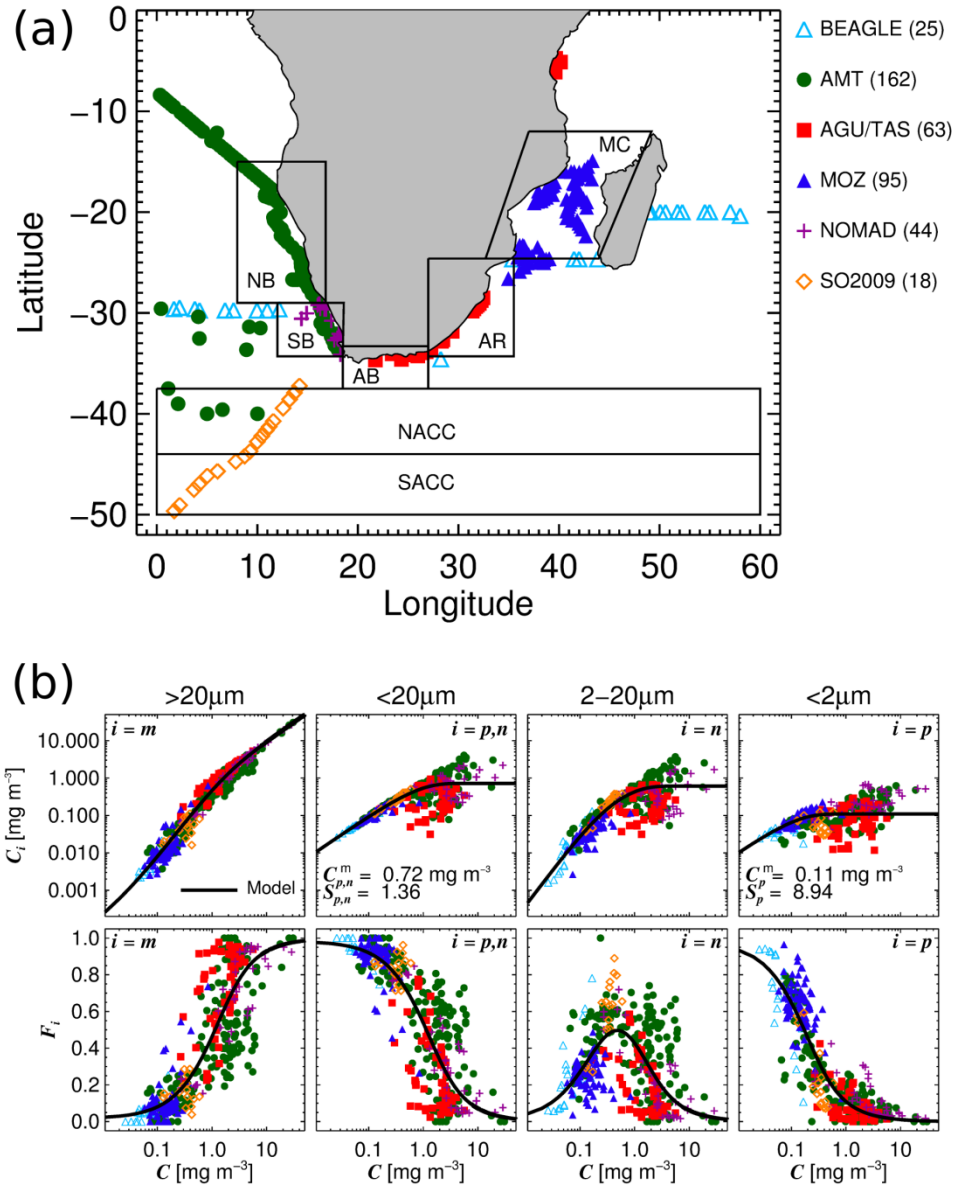

Figure 2: (a) Distribution of *in situ* pigment data used to re-tune the Brewin et al. (2010) three-component model to Southern African waters, including data from the BEAGLE cruise, the Atlantic Meridional Transect (AMT), the Agulhas ecosystem and Tanzania (AGU/TAS), the Mozambique Channel (MOZ), the NASA bio-Optical Marine Algorithm Dataset (NOMAD), and a cruise in the Atlantic sector of the Southern Ocean (SO2009). The numbering in parentheses indicates the number of samples used in each cruise. The demarcated regions follow those shown in Fig. 1. **(b)** The top row shows size-fractionated chlorophyll (C_p, $C_{p,n}$, C_n, and C_m) as a function of total chlorophyll (C), and the bottom row

185 shows the fractions (F_p, $F_{p,n}$, F_n, and F_m) as a function of total chlorophyll (C), for the *in situ*
186 parameterisation dataset (374 samples, symbols follow that of **(a)** with the regionally-tuned
187 three-component model overlain. The re-tuned parameters of the three-component model are
188 provided, with: $C_{p,n}^m$ representing the upper bound of chlorophyll for cells < 20 μm; C_p^m
189 representing the upper bound of chlorophyll for cells < 2 μm; $S_{p.n}$ representing the initial
190 slope dictating the increase in chlorophyll for cells < 20 μm as a function of total chlorophyll;
191 and S_p representing the initial slope dictating the increase in chlorophyll for cells < 2 μm as a
192 function of total chlorophyll (see Brewin et al. 2010).
193
194 Samples were matched to daily, level 3 (4 km binned) satellite chlorophyll data, from
195 MODIS-Aqua v2014.0 (downloaded from the Ocean Biology Processing Group (OBGP) at
196 NASA's Goddard Space Flight Center (GSFC)). Each *in situ* sample was matched in time
197 (daily temporal match-up) and space (closest latitude and longitude) with the satellite data.
198 Following Bailey and Werdell (2006), we used a multi-pixel box (3 x 3 pixel window) to
199 increase the possibility of an *in situ* measurement being available for comparison with the
200 MODIS-Aqua data. The median chlorophyll concentration of the nine pixels was considered
201 as the satellite estimate and only match-ups with 5 or more of the nine pixels, and with a
202 median coefficient of variation for remote-sensing reflectance bands between 412 and 547
203 nm of less than 0.15, were included, to ensure reasonable homogeneity of the match-up site
204 (Bailey and Werdell, 2006; Brewin et al., 2015b; Brewin et al., 2016). Following this criteria,
205 33 satellite match-ups of a possible 407 were available.
206
207 The 33 satellite match-ups were removed from the 407 samples and set aside for independent
208 validation of satellite Chla and size-fractionated Chla; leaving 374 samples for re-tuning of
209 the Brewin et al. (2010) model. To evaluate model performance, we used the correlation

coefficient (r) and the root-mean-square error (ψ). Statistical tests were performed in $\log_{10}$ space for the chlorophyll concentrations, considering chlorophyll is approximately log-normally distributed (Campbell, 1995), and in linear space for the size fractions. Following Brewin et al. (2015b), Eq. 1 and 2 were fitted to the 374 samples using a standard, nonlinear, least-squares method with relative weighting (Moré, 1978) to retrieve the model parameters (see Table 1 and Figure 2b). Model parameters were compared with the global model of Brewin et al. (2015b) and the Atlantic Ocean model of Brewin et al. (2010) in Table 1, and found to have significantly higher initial slopes ($S_{p,n}$ and S_p) than both previous studies, justifying the regional tuning of the model, and suggesting a higher contribution of smaller cells at low total Chla, though similar asymptotic maximum values (C_p^m and $C_{p,n}^m$) to the previous studies were shown. The model captures the general trends in absolute chlorophyll concentrations (C_p, $C_{p,n}$, C_n, and C_m) and fractions (F_p, $F_{p,n}$, F_n, and F_m) as a function of total chlorophyll for the Southern African dataset (Figure 2b). Statistical comparisons of modelled and *in situ* size-fractionated chlorophyll are comparable to those from Brewin et al. (2015b) for the global ocean (Table 2).

Table 1: Comparison of model parameters derived in this study, with those of Brewin et al. (2015b) for the global ocean and Brewin et al. (2010) for the Atlantic Ocean. Bracketed values show 15.9 % and 84.1 % confidence intervals (1 standard deviation) on a parameter distribution derived using 1000 bootstraps.

Model Parameter	**This study (Southern Africa)**	**Brewin et al. (2010) (Atlantic Ocean)**	**Brewin et al. (2015b) (Global Ocean)**
C_p^m	0.11 (0.10 to 0.12)	0.11	0.13
$C_{p,n}^m$	0.74 (0.67 to 0.78)	1.06	0.77

$S_{p,n}$	1.34 (1.26 to 1.49)	0.851	1.22
S_p	9.02 (8.21 to 9.39)	6.801	6.15

Table 2: Statistical comparison of model performance in this study with that from Brewin et al. (2015b). IN refers to the *in situ* dataset used to parameterise the model, and SAT the satellite validation dataset. *r* is the correlation coefficient, ψ the root-mean-square error and *N* the number of samples. The chlorophyll concentration is denoted *C*, and the subscript *m* refers to microphytoplankton, *n* nanophytoplankton and *p* picophytoplankton (*p,n* is combined nano-picophytoplankton).

Dataset (IN = in situ, SAT = satellite validation)	**Size-fractionated chlorophyll (C_i) or total chlorophyll (C)**	**This study (Southern Africa)**			**Brewin et al. (2015b) (Global Ocean, see their Fig. 6)**		
		r	**ψ**	***N***	***r***	**ψ**	***N***
IN	C_m	0.98	0.30	374	0.91	0.34	5841
IN	$C_{p,n}$	0.79	0.28	374	0.94	0.13	5841
IN	C_n	0.86	0.33	374	0.93	0.24	5841
IN	C_p	0.45	0.30	374	0.64	0.26	5841
SAT	C	0.98	0.14	33	0.88	0.25	598
SAT	C_m	0.96	0.29	33	0.86	0.41	598
SAT	$C_{p,n}$	0.91	0.18	33	0.79	0.27	598
SAT	C_n	0.95	0.25	33	0.80	0.38	598
SAT	C_p	0.41	0.32	33	0.57	0.28	598

2.2. Ocean colour data analysis

Standard monthly-averaged chlorophyll *a* (Chla) data (version 2014.0 for the period July 2002 to April 2016, and version 2014.0.1 for the period May to October 2016) from the MODIS-Aqua sensor, with a spatial resolution of 4.5 km, were provided by the OBGP at NASA's GSFC. Seasonal and monthly climatologies of Chla, for the 2002-2016 period were used to describe the large-scale seasonal variations in Chla. These climatologies were generated by averaging the data throughout the timeseries for each month of the year, as well as over a three month period for each season defined as austral summer (December, January, February), austral autumn (March, April, May), austral winter (June, July, August), and austral spring (September, October, November).

Since the ocean around Southern Africa is so extensive, with a number of different ecosystems and a wide range of Chla characteristics, specific regions were selected for further investigation (Figure 1). These regions were the northern Benguela (NB), southern Benguela (SB), Agulhas Bank (AB), Agulhas Region (AR), Mozambique Channel (MC), northern Antarctic Circumpolar region (NACC), and the southern Antarctic Circumpolar region (SACC) (Figure 1). The regions were defined based on the spatial variation in physical driving forces, including ecosystem responses such as primary and secondary production and the trophic structure of food webs (Hutchings et al., 2009; Kirkman et al., 2016). Within each of these regions, averages of the monthly climatologies of Chla, as well as the fractional contributions of micro-, nano-, and picophytoplankton were investigated. Dominance of different size classes has been associated with different Chla ranges, where microphytoplankton dominate at high Chla, nanophytoplankton at intermediate Chla, and picophytoplankton at low Chla concentrations (Aiken et al., 2007; Barlow et al., 2007; Uitz et al., 2006). For those regions around the Southern African coast (NB, SB, AB, AR, and MC),

further sub-division was performed using a Chla concentration of 1 mg m^{-3} to separate the higher biomass areas on the shelf from the open ocean regions, similar to Demarcq et al. (2007).

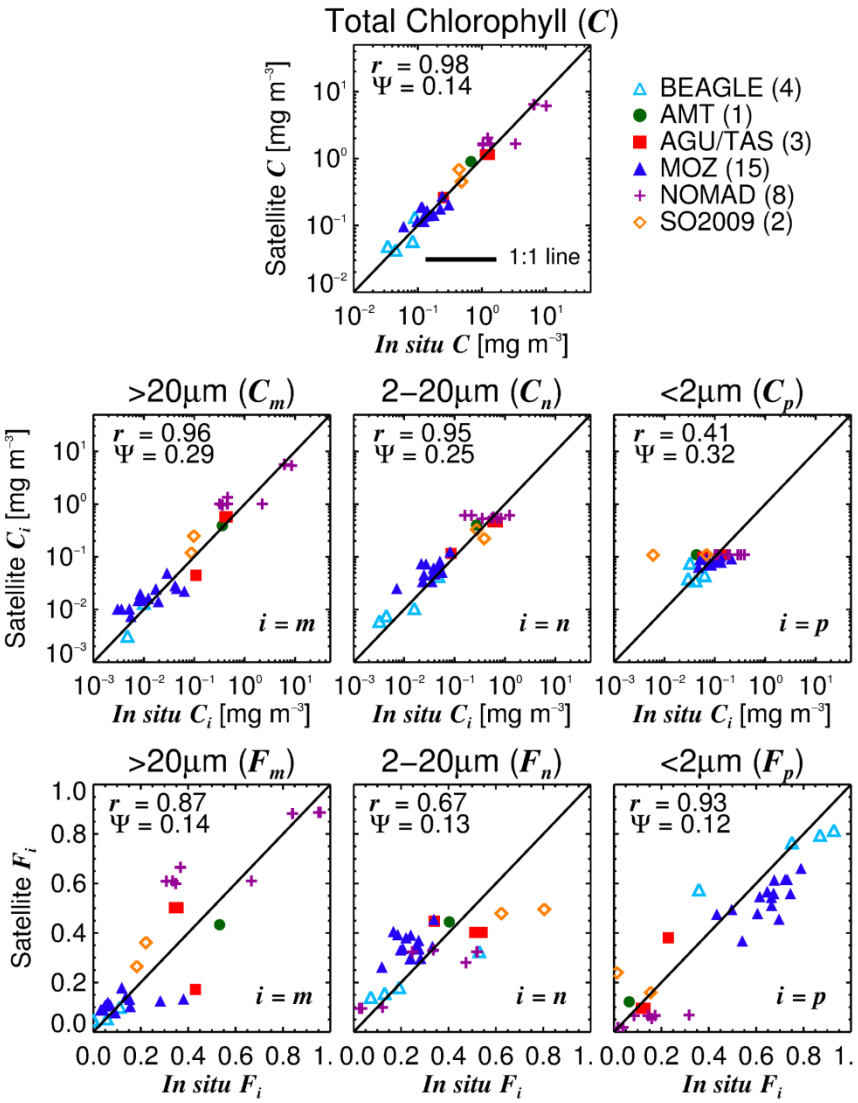

Figure 3: Independent satellite validation of total chlorophyll from MODIS-Aqua (*C*, top figure), size-fractionated chlorophyll (middle row), and the fractions of each size class to total chlorophyll (bottom row), in Southern African waters. *r* is the correlation coefficient and ψ the root-mean-square error. For the concentrations, statistical tests were performed in $\log_{10}$-space and for the fractions (bottom row), linear space.

3. Results

3.1. Satellite validation of total and size-fractionated chlorophyll

Satellite estimates of total chlorophyll are in good agreement with *in situ* data, with a high correlation coefficient and low root mean square error (Figure 3 and Table 2). In fact, the root mean square (ψ = 0.14) is considerably lower and correlation (r = 0.98) higher than that reported in other studies using global datasets (Bailey and Werdell, 2006; Brewin et al., 2015b; Gregg and Casey, 2004), and comparable with a recent study in the Atlantic Ocean using underway spectrophotometry (Brewin et al., 2016). Satellite estimates of size-fractionated chlorophyll (Figure 3 and Table 2), and the fractions of each size class to total chlorophyll (Figure 3) using the re-tuned model of Brewin et al. (2010), are also shown to compare well with the *in situ* data (r = 0.41 to 0.96). Low root mean square errors for both the satellite estimates of size-based concentrations (ψ < 0.32) and the fractions (ψ < 0.14) were found (Figure 3). These statistics are generally better than those presented by Brewin et al. (2015b) for a global validation (see Table 2). Results from this independent validation give confidence in the use of MODIS-Aqua total chlorophyll and size-fractioned chlorophyll products for Southern African waters.

3.2. Seasonal cycle of total chlorophyll and the size fractions

Seasonal Chla climatologies (Figure 4) illustrated that Chla values > 1 mg m^{-3} were limited to the shelf regions along the coasts of Southern Africa and Madagascar, while the lowest values (< 0.1 mg m^{-3}) occurred over most of the open ocean between the equator and ~ 38 °S during austral summer (Figure 4a) and autumn (Figure 4b). During austral winter and spring, Chla values up to 0.5 mg m^{-3} extended over a much larger area of the open ocean, with low values (< 0.1 mg m^{-3}) restricted to smaller regions within the subtropical gyres (Figure 4c, d).

Microphytoplankton comprised > 50 % of the total Chla in the shelf regions of Southern Africa and Madagascar, with < 20 % in the subtropical gyres and the Mozambique Channel (Figure 5 a-d), while the converse was observed for picophytoplankton (Figure 5 i-l). Notably, nanophytoplankton tended to dominate in smaller zones along the edges of the continental shelves and in the Southern Ocean between 38-44°S (Figure 5 e-h). Since the seasonally-averaged proportion of nanophytoplankton did not exceed 50 %, the 0.47 contour was chosen to delineate the regions where nanophytoplankton contributed substantially to the total Chla (Figure 5 e-h).

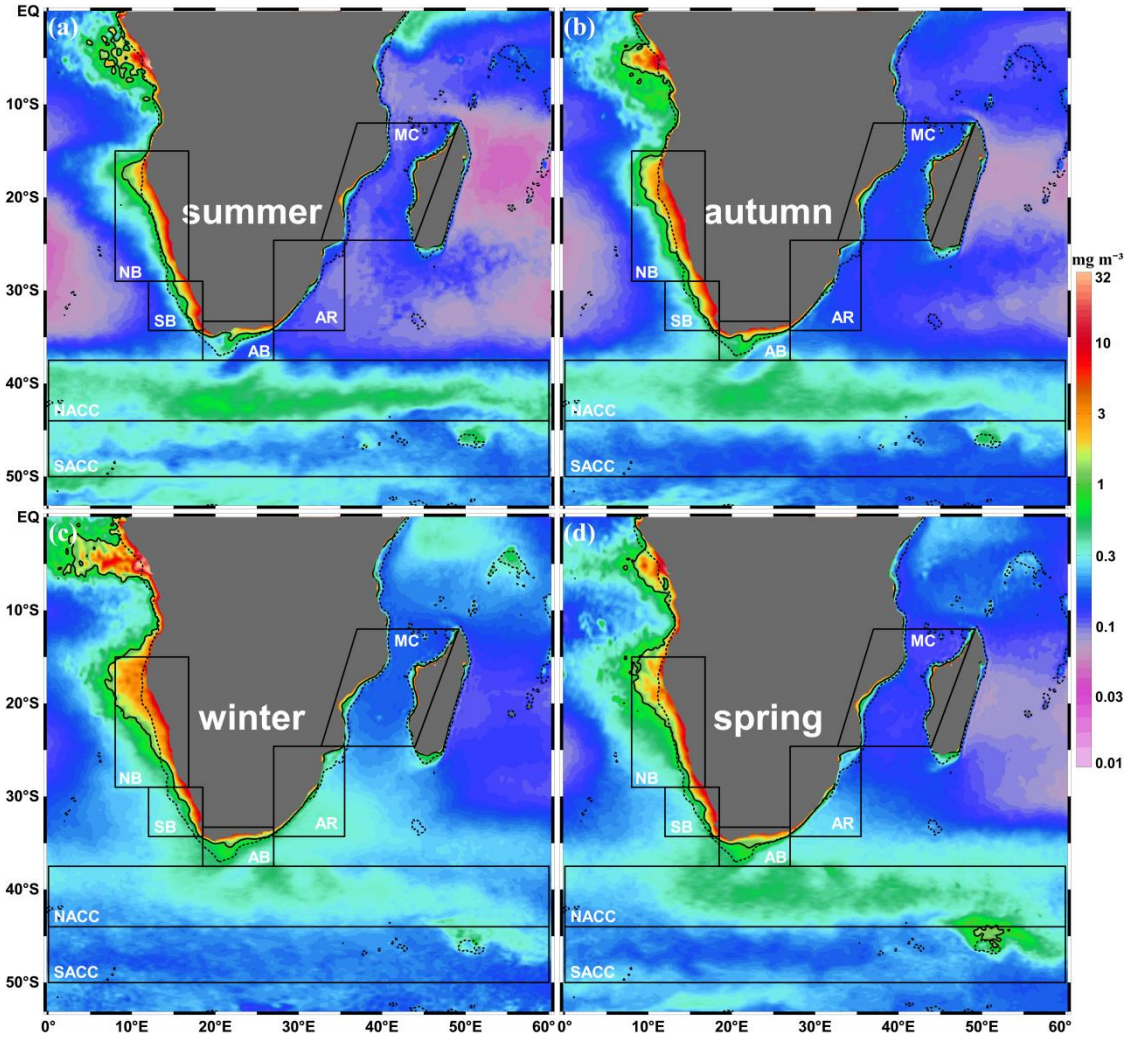

Figure 4: Seasonal climatologies (2002-2016) of MODIS-Aqua chlorophyll *a* (mg m^{-3}) during austral **(a)** summer, **(b)** autumn, **(c)** winter, and **(d)** spring. Black solid contour indicates the 1 mg m^{-3} isoline. Dotted black contours indicate the GEBCO 1000 m isobaths

(Becker et al., 2009), and the black boxes indicate the demarcated regions (NB – Northern Benguela, SB – Southern Benguela, AB – Agulhas Bank, AR – Agulhas Region, MC – Mozambique Channel, NACC – Northern Antarctic Circumpolar Current region, SACC – Southern Antarctic Circumpolar Current region).

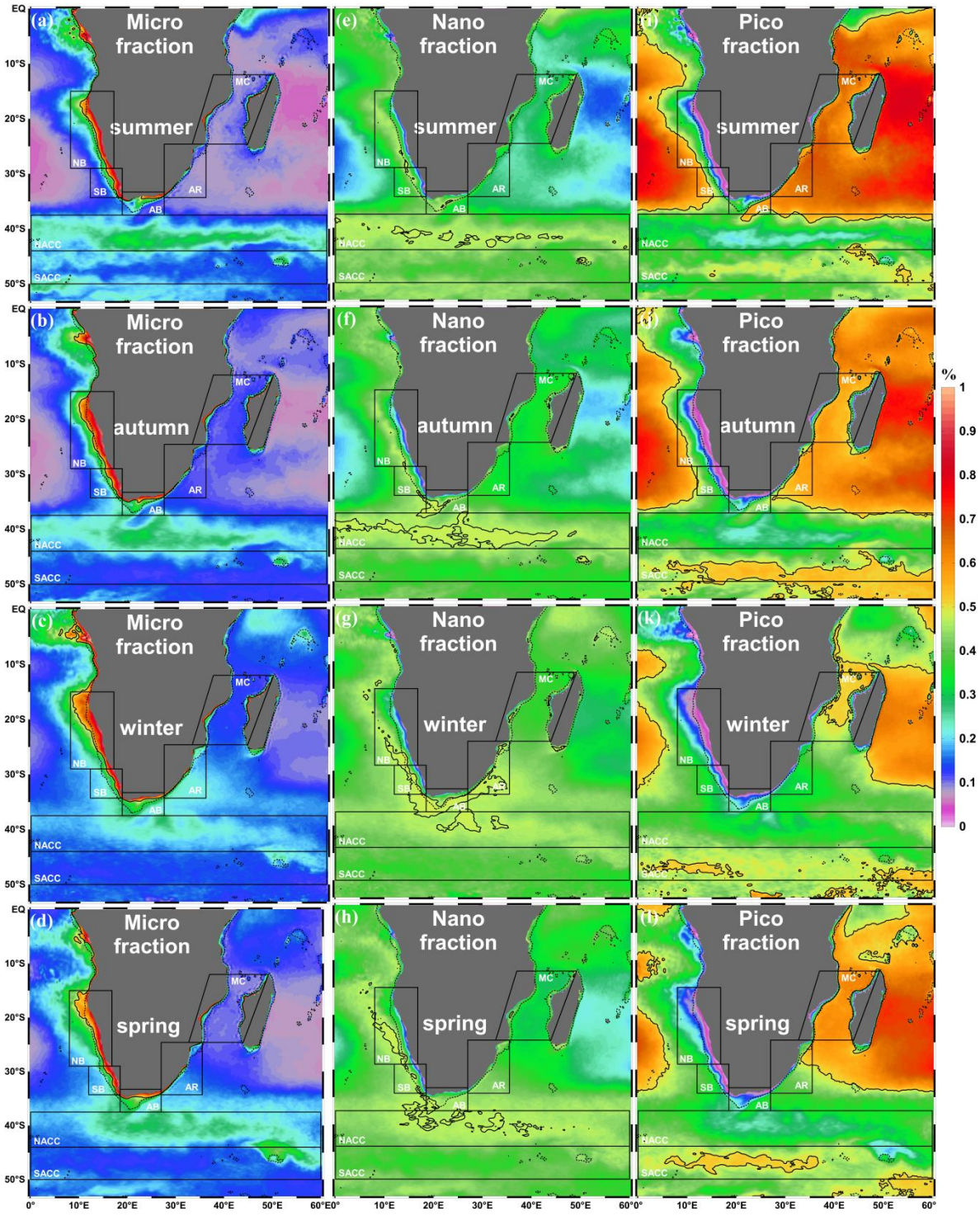

Figure 5: Seasonal climatologies (2002-2016) of the fractional contributions of **(a-d)** micro-, **(e-h)** nano-, and **(i-l)** picophytoplankton to the total MODIS-Aqua chlorophyll *a* during austral summer, autumn, winter, and spring. Black solid contours indicate the 0.5 (50 %) contour for micro- and picophytoplankton, and the 0.47 (47 %) isolines for nanophytoplankton. Dotted black contours indicate the GEBCO 1000 m isobaths (Becker et

al., 2009), and the black boxes indicate the demarcated regions (NB – Northern Benguela, SB – Southern Benguela, AB – Agulhas Bank, AR – Agulhas Region, MC – Mozambique Channel, NACC – Northern Antarctic Circumpolar Current region, SACC – Southern Antarctic Circumpolar Current region).

The shelf regions, particularly along the west and south coasts of Southern Africa, exhibited regional differences in the offshore extent of Chla concentrations > 1mg m^{-3} (Figure 4). In the northern Benguela (NB), around 17.5 °S, high Chla extended furthest offshore during austral winter (Figure 4c) and spring (Figure 4d), with less offshore extent in autumn (Figure 4b) and the lowest in summer (Figure 4a). Further south, off central Namibia (~ 23 °S), the greatest offshore extent also occurred in winter (Figure 4c), but the extent observed in autumn (Figure 4b) was greater than in summer (Figure 4a) and spring (Figure 4d).

Regional averages of the monthly mean Chla on the NB shelf indicated a peak in spring (September-October) and slightly elevated biomass in late summer-early autumn (Figure 6a). Throughout the year, microphytoplankton comprised 70-73 % of the total Chla in the NB shelf region, with the maximum proportion observed in April (Figures 5 and 7). Nanophytoplankton comprised 23-25 % of the total Chla, while the picophytoplankton contribution was ~ 5 %, with the highest fractions of both groups observed in July and November (Figures 5 and 7). In contrast, mean Chla in the offshore domain was much lower, with a peak in late winter-early spring (August-September) (Figure 6a), likely due to the increased offshore extent of higher Chla throughout the NB during this period (Figure 4). Although nanophytoplankton were dominant (44-46 %) throughout the year in the offshore domain (Figures 5 and 7b), seasonal differences in the proportions of micro- (19-32 %) and

picophytoplankton (22-41 %) were observed. During summer and autumn, the picophytoplankton proportion was greater than the microphytoplankton contribution, while the opposite was observed in winter and spring (Figures 5 and 7b).

In the southern Benguela (SB), maximum offshore extent of high Chla was found in autumn (Figure 4b) and summer (Figure 4a), while it was lower during spring (Figure 4d) and the least was observed in winter (Figure 4c). On the SB shelf, mean Chla was highest in spring (September-October), with a smaller peak in autumn (March-April) (Figure 6b). Similar to the NB shelf, microphytoplankton contributed 71-77 % to the total Chla on the SB shelf throughout the year, with nanophytoplankton comprising 19-24 %, and a 4-5 % contribution from picophytoplankton (Figures 5 and 7c). The highest proportion of microphytoplankton was observed in October, and during June for nano- and picophytoplankton (Figure 7). In contrast, the open ocean domain showed the lowest Chla in summer, while higher values were sustained from late autumn to spring (Figures 4 and 6b). Nanophytoplankton dominated (37-47 %) the Chla in the open ocean domain during autumn, winter, and spring, but in summer, the proportions of picophytoplankton (30-47 %) were higher (Figures 5 and 7d). In contrast to the NB open ocean domain (Figure 7b), the microphytoplankton proportion in the SB open ocean domain was much lower (16-23 %) (Figure 7d).

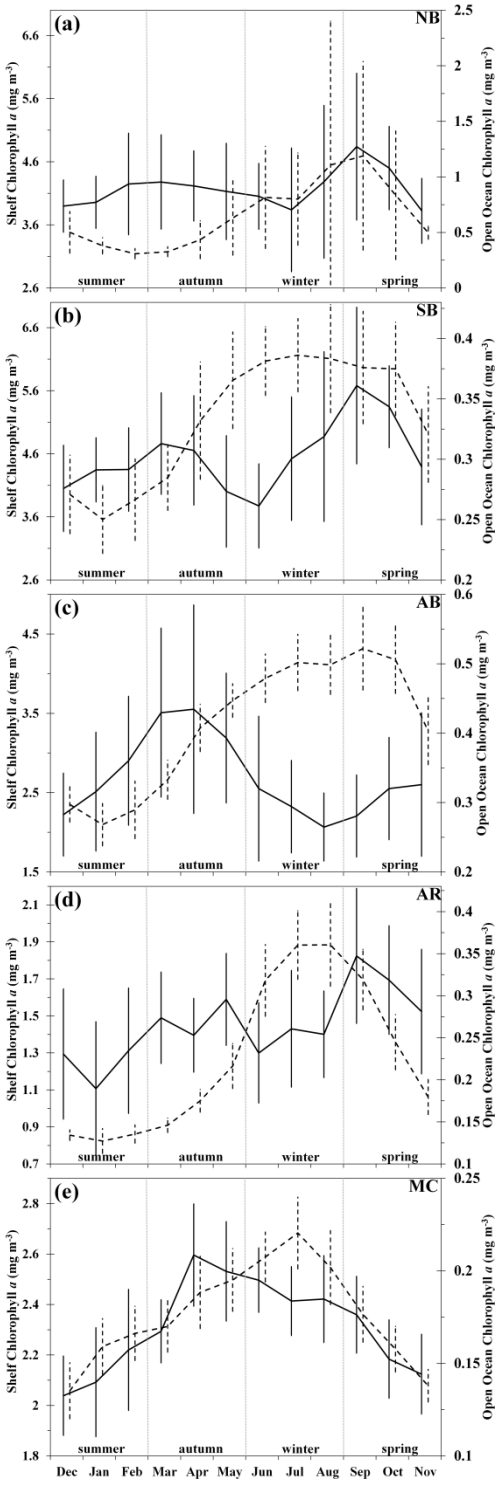

Figure 6: Monthly climatologies (2002-2016) of the mean MODIS-Aqua chlorophyll *a* (mg m^{-3}) in the **(a)** Northern Benguela (NB), **(b)** Southern Benguela (SB), **(c)** Agulhas Bank (AB), **(d)** Agulhas Region (AR), and the **(e)** Mozambique Channel (MC) regions. Black solid lines indicate shelf concentrations, while dashed lines indicate open ocean concentrations. Vertical lines indicate standard deviations of the means. Note the differences in y-axis scales.

South of Southern Africa, on the western part of the Agulhas Bank (AB), at ~ 20 °E, maximum offshore extent of high Chla occurred in winter (Figure 4c). In contrast, in the central part of the AB (~ 21.5 °E), maximum offshore extent was observed in autumn (Figure 4b), and on the eastern AB (east of 23.6 °E), it occurred in spring (Figure 4d). Throughout the AB, offshore extent of high Chla was least during summer (Figure 4a). Highest mean Chla in the shelf region was observed during autumn, while the lowest occurred in late winter (August) (Figure 6c). Similar to both the NB and SB shelf domains, microphytoplankton were also dominant (58-68 %) on the AB shelf, while the nano- (26-32 %) and picophytoplankton (6-12 %) contributions were slightly higher (Figures 5 and 7e). Peak microphytoplankton proportion was observed in April, similar to the NB region, while the nanophytoplankton contribution was highest in August, and picophytoplankton was greatest in December (Figure 7).

In contrast to the shelf, the AB open ocean region showed the lowest mean Chla in summer (January) and the highest in spring (September) (Figure 6c). Similar to the SB open ocean domain, nanophytoplankton were also dominant (39-48 %) for most of the year in the AB open ocean region, with slightly lower proportions occurring during summer (Figures 5 and 7f). Although the differences were smaller, microphytoplankton proportions exceeded the picophytoplankton contributions during winter and early- to mid-spring (Figures 5 and 7f), similar to the pattern observed in the NB open ocean region (Figure 7b).

South of ~ 31 °S, the southern part of the Agulhas region (AR), exhibited no substantial differences in the offshore extent of high Chla values (Figure 4). However, further north, in the Kwa-Zulu Natal Bight at ~ 29 °S, high Chla values extended further offshore in winter and spring (Figure 4c, d), and were restricted to a narrow area closer to the coast during

summer and autumn (Figure 4a, b). Mean Chla in the shelf region showed multiple peaks, with the highest occurring in spring (September), while the open ocean domain showed a much clearer seasonal cycle with a peak in winter (Figure 6d). On the AR shelf, higher proportions of micro- and nanophytoplankton occurred during autumn, winter, and spring. However, during summer, the picophytoplankton proportion was higher (Figures 5 and 7g). In the AR open ocean domain, picophytoplankton were dominant in mid- to late spring, and during summer and autumn, while nanophytoplankton proportions were greater in winter and early spring (Figures 5 and 7h). Although microphytoplankton contributed less than 22 % to the total Chla, the proportions were slightly higher during winter and early spring (Figures 5 and 7h).

On the Sofala Bank (~ 20 °S), in the Mozambique Channel (MC), high Chla values extended further offshore during autumn and summer (Figure 4 a, b), and were restricted closer to the coast during winter and spring (Figure 4c, d). In contrast, further northeast, along the coast of Madagascar (~ 16 °S), greater offshore extent of high Chla values occurred in winter and spring (Figure 4c, d), with less offshore extent in summer and autumn (Figure 4a, b). The shelf regions of the MC showed the highest mean Chla in autumn (April), while the open ocean region showed a peak in winter (July) (Figure 6e). In the MC shelf region, microphytoplankton comprised 56-62 % of the total Chla, while the nanophytoplankton contribution was 30-32 %, and picophytoplankton contributed 8-13 % (Figures 5 and 7i). In contrast, the MC open ocean domain showed a predominance of picophytoplankton throughout the year (Figures 5 and 7j). Microphytoplankton contributions remained below 16 % in the MC open ocean region throughout the year (Figures 5 and 7j).

In the Southern Ocean (38-44 °S), the northern Antarctic Circumpolar (NACC) region was associated with elevated Chla concentrations (up to 0.7 mg m^{-3}), with higher values occurring over a larger area in spring, summer, and autumn than during winter (Figures 4 and 8a). Throughout the year, nanophytoplankton comprised 38-46 % of the total Chla in this region, while the picophytoplankton contribution varied between 31-48 %, and the microphytoplankton proportion was 14-23 % (Figures 5 and 8b). South of 44 °S, in the southern Antarctic Circumpolar (SACC) region, Chla values were higher during mid-spring to mid-summer (Figures 4a, d and 8c), while generally lower values were observed in autumn and winter (Figure 4b, c). However, monthly mean values (Figure 8c) indicated an increase in Chla in early winter (June). Although nanophytoplankton were also prominent in the SACC (Figure 8d), and the microphytoplankton contribution was similarly low, the proportion of picophytoplankton was greater than that observed in the NACC, and exceeded the contributions of the other size fractions for most of the year (Figure 8d).

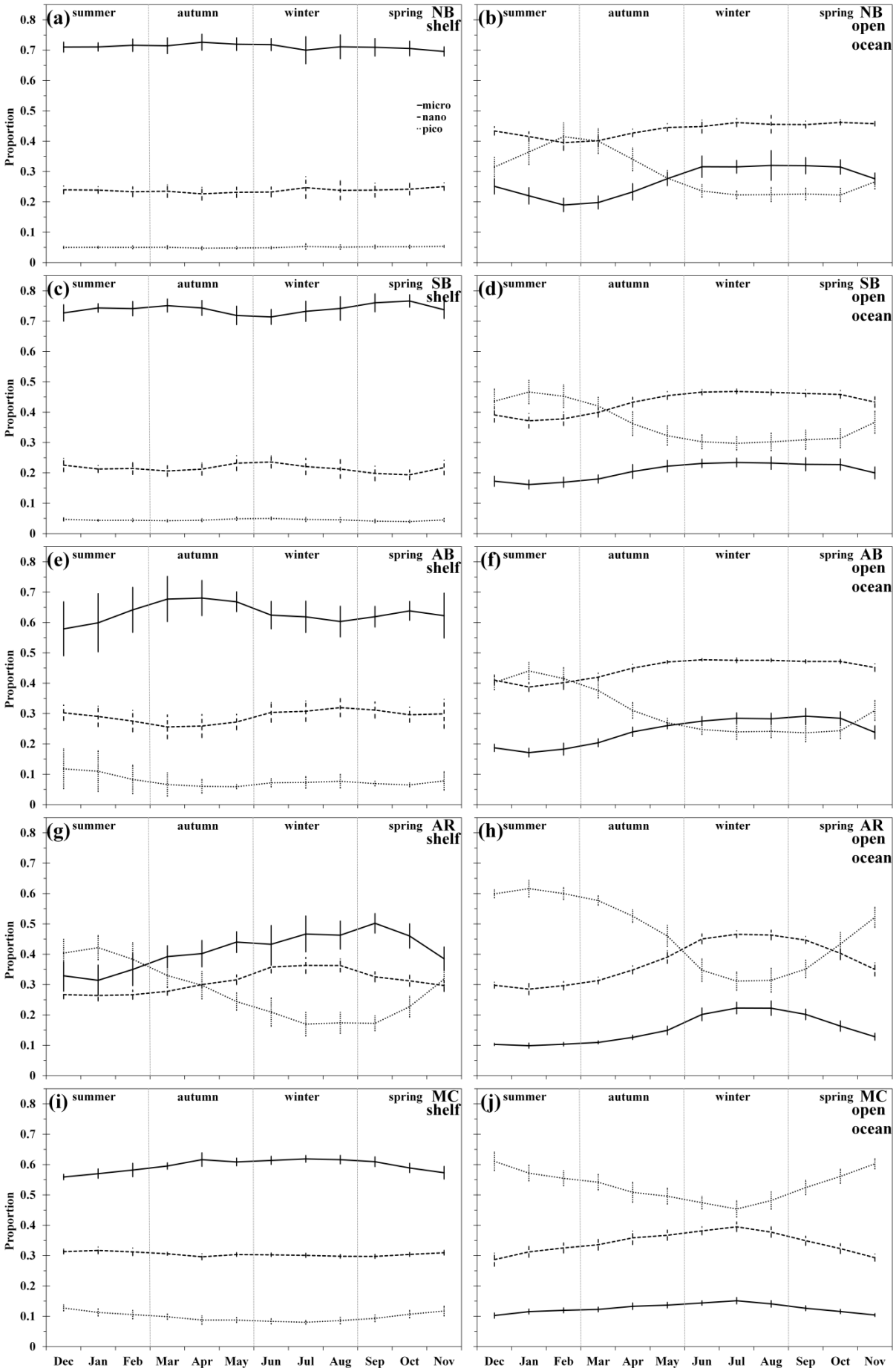
(a) summer autumn winter spring NB shelf
(b) summer autumn winter spring NB open ocean
(c) summer autumn winter spring SB shelf
(d) summer autumn winter spring SB open ocean
(e) summer autumn winter spring AB shelf
(f) summer autumn winter spring AB open ocean
(g) summer autumn winter spring AR shelf
(h) summer autumn winter spring AR open ocean
(i) summer autumn winter spring MC shelf
(j) summer autumn winter spring MC open ocean
micro
nano
pico
Proportion
0 0.1 0.2 0.3 0.4 0.5 0.6 0.7 0.8
Dec Jan Feb Mar Apr May Jun Jul Aug Sep Oct Nov

431

Figure 7: Monthly climatologies (2002-2016) of fractional contributions of micro-, nano-, and picophytoplankton to the total chlorophyll *a* in the shelf and open ocean regions of the **(a, b)** Northern Benguela (NB), **(c, d)** Southern Benguela (SB), **(e, f)** Agulhas Bank (AB), **(g, h)** Agulhas Region (AR), **(i, j)** Mozambique Channel (MC). Black solid lines indicates microphytoplankton, dashed lines indicates nanophytoplankton, and dotted lines indicates picophytoplankton contributions. Vertical lines indicate standard deviations of the means.

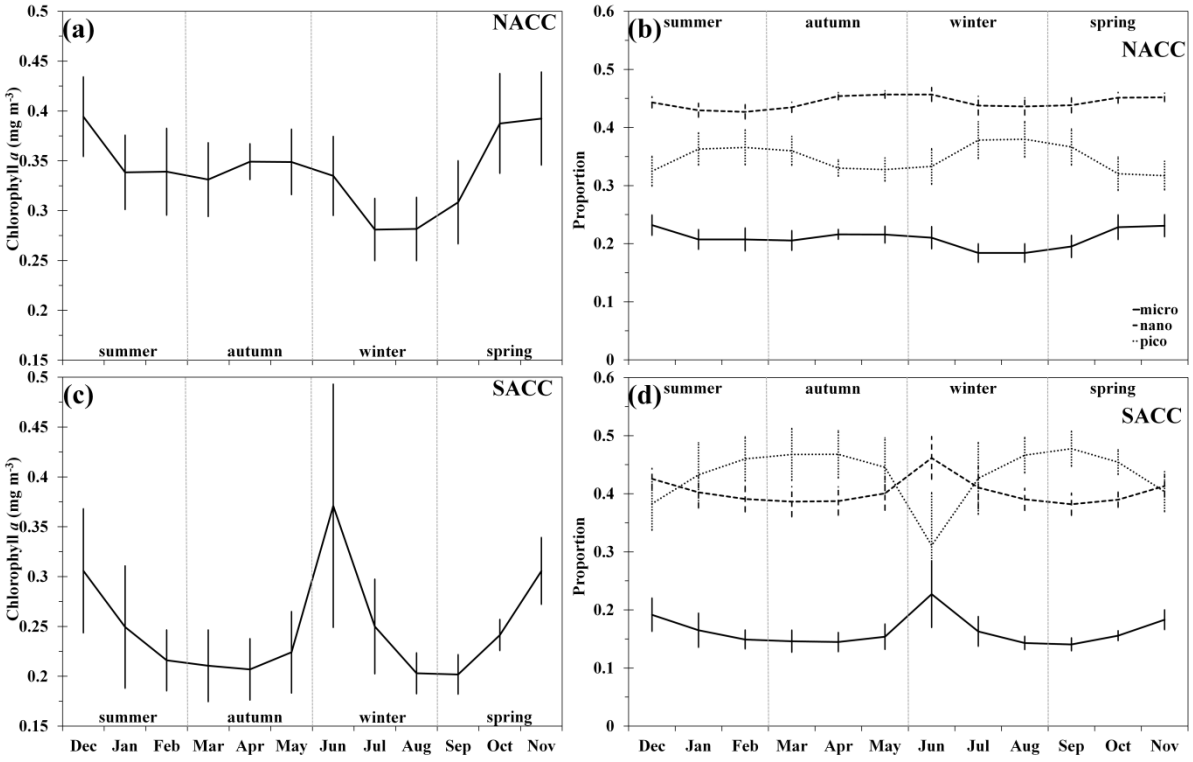

Figure 8: Monthly climatologies (2002-2016) of the mean MODIS-Aqua chlorophyll *a* (mg m^{-3}) and fractional contributions of micro-, nano-, and picophytoplankton to the total chlorophyll *a* in the **(a, b)** northern Antarctic Circumpolar Current (NACC) and **(c, d)** southern Antarctic Circumpolar Current (SACC) regions. On panels b and d, the black solid lines indicate microphytoplankton, dashed lines indicate nanophytoplankton, and dotted lines indicate picophytoplankton contributions. Vertical lines indicate standard deviations of the means.

4. Discussion

The distribution of phytoplankton populations is driven primarily by the adaptation of various communities to the availability of optimal levels of light and nutrients, which are regulated by both physical processes, including mixing and stratification, and biological processes such as growth, mortality, and grazing (IOCCG, 2014). Different phytoplankton taxa show preferences for specific environmental conditions, and they have different biogeochemical functions within an ecosystem (IOCCG, 2014). Generally, microphytoplankton tend to dominate in environments where mixing is stronger and nutrient concentrations are higher, while picophytoplankton are dominant in stratified conditions where they are better suited to utilising the regenerated nutrients found in those environments (Chisholm, 1992; Cullen et al., 2002).

Characterising and understanding the seasonal dynamics of phytoplankton size composition is critically important if we are to be able to assess the impacts of current and future climate change and variability on these populations under differing environmental conditions. Although there has been a growing number of studies investigating phytoplankton seasonality across the global ocean in recent years, such research has been lacking for marine ecosystems around Southern Africa, and thus the current study presents the first regional scale characterisation of the full seasonal cycle in satellite-derived Chla and phytoplankton size structure for this region.

4.1. West and South coast of Southern Africa

In coastal upwelling systems, such as the Benguela (including the NB, SB, and AB regions), the combined effects of variable wind forcing, nutrient input, as well as water column

mixing, stratification and retention, enhance phytoplankton growth, resulting in high biomass levels and favour the presence of micro- and nanophytoplankton (Verheye et al., 2016). These larger sized phytoplankton populations are important in driving the high productivity of this upwelling system, which supports a very rich commercial fishing and marine aquaculture industry (Kirkman et al., 2016; Verheye et al., 2016).

In the northern and southern Benguela shelf domains, surface Chla provides a reasonable indication of phytoplankton biomass distributions in the euphotic zone (Barlow et al., 2005; 2006; Louw et al., 2016; Shannon and Pillar, 1986, Lamont et al., 2014a). However, it is important to note that subsurface biomass maxima are commonly observed in the open ocean domains of the northern and southern Benguela, as well as in both the shelf and open ocean sectors of the Agulhas Bank (Barlow et al., 2005; 2006; Lamont et al., 2014b; Probyn, 1992; Shannon and Pillar, 1986), and thus, it should be recognised that satellite estimates of Chla are only representative of the surface layer. Therefore, variations of size structure presented in the current study should similarly be considered as representative of only the surface layer.

Seasonal changes and spatial variability of Chla (Figures 4 and 6) observed during the current study agreed well with the patterns described by previous investigations of satellite Chla (Demarcq et al., 2003, 2007, Verheye et al., 2016; Weeks et al., 2006). Similarly, there was good correspondence with *in situ* observations reported in previous studies. On the NB shelf, Louw et al. (2016) used a 12-year climatology of monthly *in situ* Chla in the upper 30 m of the water column and identified Chla peaks in December, April, and August, while a strong decrease was found in June and July. Likewise, on the SB shelf, *in situ* studies (Brown and Cochrane, 1991) have also documented a twofold increase in the productive area from winter to summer, and concentrations observed during spring were higher than those in autumn

(Lamont et al., 2014a). The consistency between the seasonal cycles identified in the current study and those observed in previous investigations, especially those using *in situ* data, confirms the utility of satellite Chla for examining surface phytoplankton seasonality in the region.

Notably, in the NB, SB, and AB shelf regions, the maximum offshore extent of high Chla (> 1 mg m^{-3}) was not temporally coincident with the highest mean Chla (Figures 4 and 6). The highest mean Chla was observed in spring (September) in the NB and SB regions (Figure 6a, b), while the maximum offshore extent in these regions occurred during winter and autumn, respectively (Figure 4). In the AB shelf region, the highest mean Chla occurred in autumn (April) (Figure 6c), while the maximum offshore extent varied from winter on the western AB, to autumn on the central AB, and spring on the eastern AB (Figure 4). Furthermore, the offshore extent of high microphytoplankton proportions (> 50 %) (Figure 5a-d) tended to mirror that of the high Chla (Figure 4).

It has previously been suggested that the offshore extent of high phytoplankton biomass in the NB and SB regions is controlled by the flow patterns of the Benguela Current (Demarcq et al., 2007). However, the offshore domain of the SB region is one of highly turbulent mixing, resulting from the interaction of passing anticyclonic eddies from the Agulhas Current retroflection with smaller cyclonic eddies formed within the Cape Basin (Boebel et al., 2003). Consequently, the SB region is characterised by strong gradients in eddy kinetic energy (EKE), which is very low on the shelf and very high in the offshore domain (Veitch et al., 2009). It is likely that the offshore extent of high biomass in the SB region is limited more by the strong gradients in EKE, and strong mixing offshore, than by the flow pattern of the Benguela Current. In contrast, high EKE is found much further away from the shelf in the NB

region (Veitch et al., 2009), thus allowing for further offshore extension of high biomass water in the NB as compared to the SB.

In the AB region, the offshore extent of high phytoplankton biomass is limited by the Agulhas Current. The AB shelf is relatively wide, and shallow compared to the NB and SB shelf regions (Hutchings et al., 2009). The Agulhas Current flows strongly along the shelf break, carrying warm, saline oligotrophic water, which is low in nutrients and phytoplankton biomass. Here, the inshore edge of the Agulhas Current is associated with extensive meandering, as well as the growth of shear-edge features and substantial warm water plumes, which often extend across large areas of the shelf (Lutjeharms, 2006). The interaction of this fast-flowing oligotrophic current with the comparatively slower-moving higher biomass shelf waters results in strong gradients which prevents the offshore extension of high biomass beyond the shelf edge, and also results in the southwestward advection of elevated biomass (Figures 1 and 4).

Microphytoplankton were found to dominate the high biomass areas on the NB, SB, and AB shelf regions throughout the year, with peak proportions occurring in April in the NB and AB regions, and October in the SB region (Figures 5 and 7). This is consistent with previous studies showing microphytoplankton, such as diatoms, to dominate shelf regions in upwelling systems, where temperatures are lower and nutrient concentrations are higher (Aiken et al., 2007; Barlow et al., 2001; 2005; 2006; Hirata et al., 2009; Shannon and Pillar, 1986). These microphytoplankton dominated communities can sustain higher rates of photosynthesis (Cermeño et al., 2006), as a result of their larger photosynthetic rates per unit volume (Hirata et al., 2009), and are thus very important in maintaining the high primary production in these regions. Dinoflagellates are also important in these regions, particularly in stratified waters

during late summer and early autumn (Pitcher et al., 1992; Pitcher and Nelson, 2006). The timing of peak microphytoplankton proportions in these regions is commensurate with periods of strong wind-driven upwelling and mixing which introduces nutrients into the euphotic zone, stimulating phytoplankton growth (Demarcq et al., 2007; Louw et al., 2016). Although nanophytoplankton proportions in these shelf regions were relatively low and less than 25 % on average in the NB and SB regions, their contribution to the total Chla on the AB shelf was higher (26-32 %) (Figure 7 a, c, e), reflecting greater importance of these smaller-sized phytoplankton on the AB shelf.

In contrast, in the open ocean domains of the NB, SB, and AB regions, nanophytoplankton were dominant for most of the year, except during summer, when the picophytoplankton proportion was higher (Figure 7). Nanophytoplankton, such as flagellates, have been observed to be prominent further offshore in warmer shelf waters, where they can take advantage of elevated nutrient concentrations after upwelled water has warmed (Barlow et al., 2001, 2005, 2006, 2016; Probyn, 1992), whereas picophytoplankton are most abundant in the oligotrophic open ocean regions, seaward of the oceanic front, as they are better adapted to the enhanced stratification, higher temperatures and lower nutrients found in the surface layers of these regions (Barlow et al., 2016; Brewin et al., 2010; Hirata et al., 2009).

4.2. East coast of Southern Africa and Madagascar

In comparison to the Benguela system, far fewer studies on phytoplankton have been conducted in the Agulhas region (AR), with the majority of investigations focussed on the wider shelf areas of the KwaZulu-Natal (KZN) Bight (28.5-30 °S) and the Delagoa Bight (~24-27 °S). Early studies showed Chla concentrations in Delagoa Bight ranging between 0.6 and 1.26 mg m^{-3} (Mordasova, 1980), and more recent investigations (Barlow et al. 2008;

572 Kyewalyanga et al., 2007; Sá et al., 2013) have illustrated variable phytoplankton
573 distributions in response to changing circulation patterns (Lamont et al., 2010). On the KZN
574 shelf, a wide range of *in situ* Chla concentrations has been observed (Barlow et al., 2008,
575 2010, 2013, 2015; Burchall, 1968 a, b; Carter and Schleyer, 1988). Although the variance
576 associated with these Chla values is high (Carter and Schleyer, 1988), in response to rapid
577 changes in hydrographic conditions (Lamont and Barlow, 2015; Lamont et al., 2016;
578 Lutjeharms et al., 2000), there was an indication of maximum phytoplankton biomass
579 occurring during autumn and late winter/early spring (Burchall 1968a, b; Carter and Schleyer,
580 1988).
581
582 Although the current study investigated the entire AR shelf region, higher mean Chla was
583 similarly observed during spring and autumn (Figure 6d). In this region, the Agulhas Current
584 flows strongly along the shelf edge, promoting kinematically driven upwelling at certain
585 locations (Lutjeharms et al., 2000), and is thought to drive Ekman veering along the shelf
586 slope (Lutjeharms, 2006). Deflections of the Agulhas Current from the shelf edge have been
587 observed to result in the formation of large (Tsugawa and Hasumi, 2010), as well as small
588 (Roberts et al., 2010) cyclonic eddies, embedded on the landward side of the Current. As they
589 travel southward, these eddies, as well as the Ekman veering along the shelf slope, may also
590 result in the upwelling of nutrient-rich waters onto the shelf and the subsequent stimulation of
591 phytoplankton growth (Lutjeharms, 2006). However, Lamont and Barlow (2015) have shown
592 that strong current speeds associated with the impinging of the edge of the Agulhas Current
593 onto the shelf, can result in rapid southward transport of phytoplankton biomass. The
594 multiple Chla peaks noted throughout the year in this study (Figure 6d) are thus indicative of
595 this rapidly changing environment, strongly influenced by the Agulhas Current flowing along
596 the shelf edge.

In comparison to Chla studies, investigations of size structure in the AR shelf regions have been even more infrequent, and mainly limited to individual *in situ* surveys (Barlow et al., 2008, 2010, 2013, 2015), and thus the current study represents the first study of the seasonal cycle of phytoplankton size structure in this shelf region. Although microphytoplankton was observed to dominate during autumn, winter, and spring, nanophytoplankton also contributed substantially to the total Chla from late autumn to spring (Figure 7). These periods of elevated micro- and nanophytoplankton proportions are synonymous with seasons during which wind mixing is enhanced and nutrient supply to the surface layers are greater.

These results are consistent with a previous study in the Delagoa Bight, where nanophytoplankton were observed to dominate across most of the Bight, while picophytoplankton accounted for < 20 % of the total Chla during late winter (Barlow et al., 2008). There are also some similarities with studies further south, on the KZN Bight, where micro- and nanophytoplankton communities were observed to dominate the near-shore regions in summer and winter (Barlow et al., 2013, 2015), while picophytoplankton tended to dominate along the outer edges of the KZN Bight, where the influence of the warmer Agulhas Current water was greatest (Barlow et al., 2008; 2010; 2015).

However, in striking contrast to summer observations on the shelf of the KZN Bight (Barlow et al., 2013, 2015), the current study showed that picophytoplankton was dominant in the larger AR shelf region during summer (Figure 7), likely due to the reduced wind mixing and stronger thermal stratification which results in less nutrient supply to the surface layers during this season (Lutjeharms, 2006). The AR region is the only shelf region along the Southern African coast where the seasonality in phytoplankton size structure closely

resembles that of the open ocean domains (Figure 7), suggesting strong influence of offshore dynamics on the shelf ecosystem. Agulhas Current surface waters are generally very warm, saline, and nutrient-poor (Lutjeharms 2006; Barlow et al., 2013, 2015). These oligotrophic conditions favour the presence of smaller-sized phytoplankton as they are better suited to utilising the regenerated nutrients available in these surface waters (Barlow et al., 2015). This disparity to other shelf regions is likely also enhanced by the effect of averaging over a larger area in the current study (see Figure 1 for extent of the AR region), which includes the region south of 31 °S where the shelf is very narrow and the edge of the Agulhas Current is able to impinge much closer to the coast (Lutjeharms, 2006).

Similar to the AR region, there have been few studies of the large scale variations in phytoplankton biomass and size structure in the MC region. In particular, studies on the shelf region have been historically very limited, despite the ecological and economic significance of the ecosystem to local fisheries (Leal et al., 2009). The current study showed that in the MC shelf region, peak Chla was observed in April (Figure 6e), and that microphytoplankton were dominant throughout the year (Figure 7i), and suggest that there is little seasonal change in the size structure on the MC shelf (Figure 6e). On the Sofala Banks, where the shelf is wide and relatively shallow (Lutjeharms, 2006), higher biomass levels and microphytoplankton dominance was limited to the inner part of the shelf (Figures 1, 4, and 5), where river and estuarine discharge are known to enhance nutrient concentrations in the surface layers (Leal et al., 2009).

In contrast, the outer part of the shelf was dominated by nanophytoplankton communities (Figure 5), likely due to the enhanced nutrient conditions in the surface layers resulting from the upwelling induced by the interaction of offshore mesoscale features with the shelf edge.

These findings are also consistent with a previous study by Sá et al. (2013), which showed that during summer, micro- and nanophytoplankton communities dominated in cooler waters, while picophytoplankton were prevalent in warmer waters on the shelf. On the southern Madagascar shelf region, Pripp et al. (2014) observed elevated Chla values associated with wind-driven upwelling, whereas elevated Chla in the northern region at 16 °S appeared to be driven by upwelling induced by the interaction of anti-cyclonic eddies with the shelf.

Chla variability in the northern (10-16 °S) and southern (24-30 °S) sectors of the open ocean domain in the Mozambique Channel (MC) is characterised by the predominance of the seasonal cycle, with Chla reaching a peak in July-August (Lévy et al., 2007; Tew Kai and Marsac, 2009). In contrast, in the central (16-24 °S) portion of the MC, Tew Kai and Marsac (2009) demonstrated that Chla variations are driven by intense mesoscale dynamics, with anti-cyclonic eddies associated with low Chla values, while elevated Chla was related to cyclonic eddies. Subsurface phytoplankton biomass maxima are common in both the shelf and open ocean sectors of the Agulhas region and the Mozambique Channel (Barlow et al., 2014; 2015; Lamont et al., 2015; Sá et al., 2013) and thus the variations in Chla and size structure presented in the current study are representative of the surface layer only.

It has been suggested that eddy formation in the MC displays a seasonal cycle, in relation to variability in the South Equatorial Current north of Madagascar, with maxima occurring during winter, and minima in summer (Backeberg and Reason, 2010). These mesoscale eddies are known to interact with the shelf, resulting in locally enhanced upwelling and increases in phytoplankton biomass, and can also cause entrainment and export of chlorophyll-rich water from the shelf to the open ocean (Barlow et al., 2014; Lamont et al., 2014b; Quartly and Srokosz, 2004; Ridderinkhof and de Ruijter, 2003; Schouten et al., 2003).

In this study, averaged Chla values across the entire MC open ocean region (Figure 6e) displayed a maximum in winter (July), similar to observations by Tew Kai and Marsac (2009), and also corresponded with the seasonality in eddy formation suggested by Backeberg and Reason (2010).

In contrast to the other open ocean domains in the regions around Southern Africa, the MC open ocean domain showed dominance of picophytoplankton throughout the year (Figure 7j). The elevated picophytoplankton proportions during late austral spring to early austral summer (Figure 7j) may be related to the seasonal influx of chlorophyll-poor subtropical surface waters from the south Indian Ocean gyre into the Mozambique Channel (Schouten et al., 2005). These findings are in agreement with previous studies which showed that surface phytoplankton populations in the MC open ocean domain are comprised primarily of picophytoplankton, with nanophytoplankton being of secondary importance during summer and autumn (Barlow et al., 2007; 2014; Zubkov and Quartly, 2003).

4.3. Southern Ocean

South of the African continent, the Southern Ocean generally exhibits relatively low Chla (Figures 1 and 4), despite the large concentrations of unused macronutrients such as nitrate and phosphate in the surface layers (Moore and Abbott, 2002). Although satellite Chla in the Southern Ocean is significantly underestimated compared to *in situ* measurements (Kahru and Mitchell, 2010), surface Chla values are considered to be representative of the biomass in the upper mixed layer (Arrigo et al., 2008; Thomalla et al., 2011a). It is widely accepted that these low phytoplankton biomass levels are maintained by a variety of forcing mechanisms, among which the key factors are water column stability, and the availability of light and micronutrients such as iron and silicic acid (Arrigo et al., 2008; Behrenfeld, 2010).

Throughout the Southern Ocean, the seasonal variations in phytoplankton biomass are strongly controlled by the seasonal cycle of solar irradiance, which governs light availability and also impacts water column stability, and hence nutrient supply to the surface layers, through changes in the net heat flux (Arrigo et al., 2008; Swart et al., 2015). These conditions favour the dominance of picophytoplankton, which are better adapted to take advantage of such light and nutrient conditions (Laubscher et al., 1993; Perissinotto et al., 1990). This is particularly clear in the SACC region, where picophytoplankton were dominant throughout the year, except in late spring and early summer when nanophytoplankton proportions were slightly more elevated (Figures 5 and 8). However, a study by Thomalla et al. (2011a) revealed a more complex pattern of regional variations in the seasonal expression of Chla, implying distinct regional differences in the mechanisms supplying light and iron to the surface layers.

Exceptions to this general pattern of low Chla commonly occur in the vicinity of sub-Antarctic islands where the bathymetry is shallower and phytoplankton biomass is elevated as a result of the "island mass effect" (McQuaid and Froneman, 2008). This is especially evident in the vicinity of the Prince Edward and Crozet Island archipelagos, located in the SACC region, where elevated Chla concentrations and higher proportions of micro- and nanophytoplankton were observed throughout the year (Figures 1, 4, and 5). Elevated Chla concentrations are also associated with the major fronts and mesoscale activity of the Antarctic Circumpolar Current due to increased micro- and macronutient concentrations and improved light conditions, resulting from the shoaling of the upper mixed layer (Lutjeharms et al., 1985; Moore and Abbott, 2002; Thomalla et al., 2011a, b; Swart et al., 2015).

In the NACC region, the Subtropical Front (STF, 41.6 ± 1.07 °S) separates warmer subtropical surface waters from the sub-Antarctic region, while the Sub-Antarctic Front (SAF, 46.4 ± 1.07 °S) delineates the northern boundary of the Antarctic Polar Frontal Zone (APFZ) (Durgadoo et al., 2010, Lutjeharms and Valentine, 1984). Due to the location of both these fronts in the NACC region, Chla concentrations (Figures 4 and 8a, b) and the proportions of nano- and microphytoplankton (Figures 5 and 8b, c) were higher than those observed in the SACC region. This is in agreement with previous observations which also identified elevated Chla in this region, particularly during spring and summer (Gibberd et al., 2013; Thomalla et al., 2011b; Swart et al., 2015). Although monthly mean Chla indicated an increase in the SACC region in June (Figure 8c), and there appeared to be an increase in the proportion of nanophytoplankton relative to the picophytoplankton (Figure 8d), this should be viewed with caution, since this apparent increase is likely to be an artifact resulting from a lack of data coverage over much of this region during winter, particularly in June (Thomalla et al., 2011a).

5. Summary

When fitting the three-component model (Brewin et al., 2010) to data around Southern Africa, we found significantly higher initial slopes ($S_{p,n}$ and S_p) in model parameters than previous studies using global or Atlantic-basin datasets (Brewin et al., 2010; 2015b), indicating a higher concentration of Chla for small cells at low total Chla concentrations when compared to global models. This suggests a slightly different relationship between phytoplankton size structure and total Chla in this region. The satellite-derived seasonal cycles of Chla and size structure observed in the current study compared well to previously observed variations in each of the regions, suggesting that the three-component model

747 (Brewin et al., 2010) captures the spatial and seasonal variations in phytoplankton size
748 structure in the region around Southern Africa, and may provide worthwhile information for
749 observing longer-term variability of phytoplankton communities.
750
751 The NB, SB, and AB shelf regions form part of the highly productive wind-driven Benguela
752 upwelling system, while the MC shelf region comprises part of the northern reaches of the
753 oligotrophic greater Agulhas Current system. Despite the large differences in physical forcing
754 and biological characteristics in these regions, the shelf domains of the NB, SB, AB, and MC
755 regions all showed a similar seasonal cycle of phytoplankton size structure, with a dominance
756 of microphytoplankton, and very little change throughout the year. Unlike these regions, the
757 AR shelf domain was the only one where a seasonal change in the dominant phytoplankton
758 group was observed, with picophytoplankton dominating in summer, and micro- and
759 nanophytoplankton the rest of the year. The open ocean domains of the NB, SB, AB, and AR
760 regions showed a change from picophytoplankton dominance in summer (and autumn in the
761 AR region), to nanophytoplankton dominance throughout the rest of the year. In contrast, the
762 MC open ocean domain showed picophytoplankton dominance throughout the year. In the
763 Southern Ocean, the NACC region showed dominance of nanophytoplankton throughout the
764 year, as a result of improved light and nutrient conditions associated with the STF and the
765 SAF, while, in contrast, the SACC region showed picophytoplankton dominance for most of
766 the year, except in June, November, and December.
767
768 Climate change has had a substantial impact on marine ecosystems globally, and is predicted
769 to continue to modify the seasonal dynamics of physical and biological processes and
770 ecosystem responses (Doney et al., 2012). The large scale warming trends which have been
771 observed in most ecosystems (Belkin, 2009) have already resulted in substantial spatial

changes in global phytoplankton distributions, as well as a reduction in global primary production since the 1990s (Gregg and Rousseaux, 2014; Behrenfeld et al., 2006; 2016). Furthermore, alterations in food web structure and ecosystem functioning are expected as increased thermal stratification and reduced nutrient supply to the surface layers would favour the proliferation of smaller-sized phytoplankton communities (Hofmann and Todgham, 2010; O'Connor et al., 2009; Verheye et al., 2016). This study showed that nano- and picophytoplankton are the most abundant groups in the offshore marine region around Southern Africa, while microphytoplankton are more prevalent in shelf regions. In the context of a warming climate, it is likely that these microphytoplankton dominated shelf regions would change to a system where smaller groups are more prevalent, thus significantly altering ecosystem functioning in these ecologically and economically important regions.

Phytoplankton populations have high turnover rates which are strongly coupled to environmental variations, making them ideal indicators to elucidate biological responses to environmental forcing (Platt and Sathyendranath, 2008). In the context of studying the ocean carbon cycle and detecting climate change, it has been recognised that different phytoplankton taxa have different biogeochemical functions within an ecosystem (IOCCG, 2014), and for this reason, the composition and structure of phytoplankton populations have become increasingly important as ecological indicators to assess ecosystem functioning, and their detection from remotely-sensed data enables the study of seasonal and inter-annual variations, as well as long-term trends in these indicators (Platt and Sathyendranath, 2008). Application of a regionally-tuned PFT algorithm to remotely-sensed chla in this study provides the first regional scale characterisation of the full seasonal cycle in phytoplankton size structure for this region, and has revealed substantial seasonal and spatial variations in size structure under widely differing environmental conditions around Southern Africa. These

observations provide a baseline against which inter-annual and longer-term variations in phytoplankton can be assessed.

Acknowledgements

Monthly-averaged MODIS-Aqua chlorophyll *a* concentrations were provided by the Ocean Biology Processing Group (OBGP) at NASA's Goddard Space Flight Center (GSFC). (NASA Goddard Space Flight Center, Ocean Ecology Laboratory, Ocean Biology Processing Group. Moderate-resolution Imaging Spectroradiometer (MODIS) Aqua Ocean Color Data; 2014 Reprocessing. NASA OB.DAAC, Greenbelt, MD, USA. doi: 10.5067/AQUA/MODIS_OC.2014.0. Accessed on 04/01/2016). RJWB was supported by the NERC National Centre for Earth Observation, and TL and RGB by the South African Department of Environmental Affairs (DEA) and the National Research Foundation (NRF).

References

Aiken, J., Fishwick, J. R., Lavender, S., Barlow, R., Moore, G. F., Sessions, H., Bernard, S., Ras, J., Hardman-Mountford, N. J. 2007. Validation of MERIS reflectance and chlorophyll during the BENCAL cruise October 2002: preliminary validation of new demonstration products for phytoplankton functional types and photosynthetic parameters. International Journal of Remote Sensing, 28, 497-516. doi:10.1080/01431160600821036.

Aiken, J., Pradhan, Y., Barlow, R., Lavender, S., Poulton, A., Holligan, P., Hardman-Mountford, N. 2009. Phytoplankton pigments and functional types in the Atlantic Ocean: A decadal assessment, 1995-2005. Deep-Sea Research II, 56, 899-917. http://dx.doi.org/10.1016/j.dsr2.2008.09.017.

Arrigo, K. R., van Dijken, G. L., Bushinsky, S. 2008. Primary production in the Southern Ocean, 1997-2006. Journal of Geophysical Research, 113, C08004, doi:10.1029/2007JC004551.

Backeberg, B. C., Reason, C. J. C. 2010. A connection between the South Equatorial Current north of Madagascar and Mozambique Channel Eddies. Geophysical Research Letters, 37, L04604, doi:10.1029/2009GL041950.

Bailey, S. W., Werdell, P. J. 2006. A multi-sensor approach for the on-orbit validation of ocean color satellite data products. Remote Sensing of Environment, 102, 12-23. http://dx.doi.org/10.1016/j.rse.2006.01.015.

Barlow, R. G., Aiken, J., Sessions, H. E., Lavender, S., Mantel, J. 2001. Phytoplankton pigment, absorption and ocean colour characteristics in the southern Benguela ecosystem. South African Journal of Science, 97, 230-238.

Barlow, R., Gibberd, M.-J., Lamont, T., Aiken, J., Holligan, P. 2016. Chemotaxonomic phytoplankton patterns on the eastern boundary of the Atlantic Ocean. Deep-Sea Research I, 111, 73-78. http://dx.doi.org/10.1016/j.dsr.2016.02.011.

Barlow, R., Kyewalyanga, M., Sessions, H., van den Berg, M., Morris, T. 2008. Phytoplankton pigments, functional types, and absorption properties in the Delagoa and Natal Bights of the Agulhas ecosystem. Estuarine, Coastal and Shelf Science, 80, 201-211. doi:10.1016/j.ecss.2008.07.022.

Barlow, R., Lamont, T., Britz, K., Sessions, H. 2013. Mechanisms of phytoplankton adaptation to environmental variability in a shelf ecosystem. Estuarine, Coastal and Shelf Science, 133, 45-57. http://dx.doi.org/10.1016/j.ecss.2013.08.006.

Barlow, R. G., Lamont, T., Gibberd, M.-J., van den Berg, M., Britz, K. 2015. Chemotaxonomic investigation of phytoplankton in the shelf ecosystem of the KwaZulu-Natal Bight, South Africa. African Journal of Marine Science, 37, 467-484. doi:10.2989/1814232X.2015.1106976.

Barlow, R., Lamont, T., Kyewalyanga, M., Sessions, H., Morris, T. 2010. Phytoplankton production and physiological adaptation on the southeastern shelf of the Agulhas ecosystem. Continental Shelf Research, 30, 1472-1486. doi:10.1016/j.csr.2010.05.007.

Barlow, R., Lamont, T., Kyewalyanga, M., Sessions, H., van den Berg, M., Duncan, F. 2011. Phytoplankton production and adaptation in the vicinity of Pemba and Zanzibar islands, Tanzania. African Journal of Marine Science, 33, 283-295. doi: 10.2989/1814232X.2011.600430.

Barlow, R., Lamont, T., Morris, T., Sessions, H., van den Berg, M. 2014. Adaptation of phytoplankton communities to mesoscale eddies in the Mozambique Channel. Deep-Sea Research II, 100, 106-118. http://dx.doi.org/10.1016/j.dsr2.2013.10.020.

Barlow, R. G., Louw, D., Balarin, M., Alheit, J. 2006. Pigment signatures of phytoplankton composition in the northern Benguela ecosystem during spring. African Journal of Marine Science, 28, 479-491. doi:10.2989/18142320609504200.

Barlow, R. G., Sessions, H., Balarin, M., Weeks, S., Whittle, C., Hutchings, L. 2005. Seasonal variation in phytoplankton in the southern Benguela: pigment indices and ocean colour. African Journal of Marine Science, 27, 275-287. doi:10.2989/18142320509504086.

Barlow, R., Stuart, V., Lutz, V., Sessions, H., Sathyendranath, S., Platt, T., Kyewalyanga, M., Clementson, L., Fukasawa, M., Watanabe, S., Devred, E. 2007. Seasonal pigment patterns of surface phytoplankton in the subtropical southern hemisphere. Deep-Sea Research I, 54, 1687-1703. doi:10.1016/j.dsr.2007.06.010.

Becker, J. J., Sandwell, D. T., Smith, W. H. F., Braud, J., Binder, B., Depner, J., Fabre, D., Factor, J., Ingalls, S., Kim, S-H., Ladner, R., Marks, K., Nelson, S., Pharaoh, A., Trimmer,

R., Von Rosenberg, J., Wallace, G., Weatherall, P. 2009. Global Bathymetry and Elevation Data at 30 Arc Seconds Resolution: SRTM30_PLUS. Marine Geodesy, 32, 355-371, doi: 10.1080/01490410903297766

Behrenfeld, M. J. 2010. Abandoning Sverdrup's critical depth hypothesis on phytoplankton blooms. Ecology, 91, 977-989. doi:10.1890/09-1207.1.

Behrenfeld, M. J., O'Malley, R. T., Boss, E. S., Westberry, T. K., Graff, J. R., Halsey, K. H., Milligan, A. J., Siegel, D. A., Brown, M. B. 2016. Revaluating ocean warming impacts on global phytoplankton. Nature Climate Change, 6, 323-330, doi:10.1038/nclimate2838.

Behrenfeld, M. J., O'Malley, R. T., Siegal, D. A., McClain, C. R., Sarmiento, J. L., Feldman, G. C., Milligan, A. J., Falkowski, P. G., Letelier, R. M., Boss, E. S. 2006. Climate-driven trends in contemporary ocean productivity. Nature, 444, 752-755, doi:10.1038/nature05317.

Belkin, I. M. 2009. Rapid warming of Large Marine Ecosystems. Progress in Oceangraphy, 81, 207-213. doi:10.1016/j.pocean.2009.04.011.

Boebel, O., Lutjeharms, J., Schmid, C., Zenk, W., Rossby, T., Barron, C. 2003. The Cape Cauldron: a regime of turbulent inter-ocean exchange. Deep-Sea Research, 50, 57-86. doi: 10.1016/S0967-0645(02)00379-X

Brewin, R. J. W., Dall'Olmo, G., Pardo, S., van Dongen-Vogels, V., Boss, E. S. 2016. Underway spectrophotometry along the Atlantic Meridional Transect reveals high

909 performance in satellite chlorophyll retrievals. Remote Sensing of Environment, 183, 82-97.
910 doi:10.1016/j.rse.2016.05.005.
911
912 Brewin, R. J. W., Hardman-Mountford, N. J., Lavender, S. J., Raitsos, D. E., Hirata, T., Uitz,
913 J., Devred, E., Bricaud, A., Ciotti, A., Gentili, B. 2011. An intercomparison of bio-optical
914 techniques for detecting dominant phytoplankton size class from satellite remote sensing.
915 Remote Sensing of Environment, 115, 325-339. doi:10.1016/j.rse.2010.09.004.
916
917 Brewin, R. J. W., Hirata, T., Hardman-Mountford, N. J., Lavender, S. J., Sathyendranath, S.,
918 Barlow, R. 2012. The influence of the Indian Ocean Dipole on interannual variations in
919 phytoplankton size structure as revealed by Earth Observation. Deep-Sea Research II, 77-80,
920 117-127, doi: 10.1016/j.dsr2.2012.04.009.
921
922 Brewin, R. J. W., Raitsos, D. E., Dall'Olmo, G., Zarokanellos, N., Jackson, T., Racault, M.-
923 F., Boss, E., Sathyendranath, S., Jones, B. H., Hoteit, I. 2015a. Regional ocean-colour
924 chlorophyll algorithms for the Red Sea. Remote Sensing of Environment, 165, 64-85, doi:
925 10.1016/j.rse.2015.04.024.
926
927 Brewin, R. J. W., Sathyendranath, S., Hirata, T., Lavender, S., Barciela, R. M, Hardman-
928 Mountford, N. J. 2010. A three-component model of phytoplankton size class for the Atlantic
929 Ocean. Ecological Modelling, 221, 1472-1483. http://dx.doi.org/10.1016/j.rse.2015.07.004.
930
931 Brewin, R. J. W., Sathyendranath, S., Jackson, T., Barlow, R., Brotas, V., Airs, R., Lamont,
932 T. 2015b. Influence of light in the mixed layer on the parameters of a three-component model

933 of phytoplankton size structure. Remote Sensing of Environment, 168, 437-450, doi:
934 10.1016/j.rse.2015.07.004.
935
936 Brewin, R. J. W., Sathyendranath, S., Tilstone, G., Lange, P. K., Platt, T. 2014. A
937 multicomponent model of phytoplankton size structure. Journal of Geophysical Research –
938 Oceans, 119, 3478-3496, doi:10.1002/2014JC009859.
939
940 Brito, A. C., Sá, C., Brotas, V., Brewin, R. J. W., Silva, T., Vitorino, J., Platt, T.,
941 Sathyendranath, S. 2015. Effect of phytoplankton size classes on bio-optical properties of
942 phytoplankton in the Western Iberian coast: Application of models. Remote Sensing of
943 Environment, 156, 537-550, doi:10.1016/j.rse.2014.10.020.
944
945 Brotas, V., Brewin, R. J. W., Sá, C., Brito, A. C., Silva, A., Mendes, C. R., Diniz, T.,
946 Kaufmann, M., Tarran G., Groom, S. B., Platt, T., Sathyendranath, S. 2013. Deriving
947 phytoplankton size classes from satellite data: Validation along a trophic gradient in the
948 eastern Atlantic Ocean. Remote Sensing of Environment, 134, 66-77, doi:
949 10.1016/j.rse.2013.02.013.
950
951 Brown, P. C., Cochrane, K. L. 1991. Chlorophyll *a* distribution in the southern Benguela:
952 Possible consequences of global warming on phytoplankton and its implications for pelagic
953 fish. South African Journal of Science, 87, 233-242.
954
955 Burchall, J. 1968a. Primary production studies in the Agulhas Current region off Natal –
956 June, 1965. Investigational Report No. 20. Durban: Oceanographic Research Institute.
957

Burchall, J. 1968b. An evaluation of primary productivity studies in the continental shelf region of the Agulhas Current near Durban (1961-1966). Investigational Report No. 21. Durban: Oceanographic Research Institute.

Campbell, J. W. 1995. The lognormal distribution as a model for bio-optical variability in the sea. Journal of Geophysical Research, 100 (C7), 13237-13254. http://dx.doi.org/10.1029/95JC00458.

Carter, R. A., Schleyer, M. H. 1988. Phytoplankton distributions in Natal coastal waters. In: Schumann, E. H. (Ed.), Coastal ocean studies off Natal, South Africa. Lecture Notes on Coastal and Estuarine Studies, 26. Berlin, Springer-Verlag. pp. 152-177.

Cermeño, P., Marañón, E., Pérez, V., Serret, P., Fernández, E., Castro, C. G. 2006. Phytoplankton size structure and primary production in a highly dynamic coastal ecosystem (Ría de Vigo, NW-Spain): Seasonal and short-time scale variability. Estuarine Coastal and Shelf Science, 67, 251-266. doi:10.1016/j.ecss.2005.11.027.

Chisholm, S. W. 1992. Phytoplankton size. In: Falkowski, P. G., Woodhead, A. D. (Eds.), Primary Productivity and Biogeochemical Cycles in the Sea. Springer, New York, pp. 213-237.

Cullen, J. J., Franks, P. J. S., Karl, D. M., Longhurst, A. 2002. Physical influences on marine ecosystem dynamics. In: Robinson, A. R., McCarthy, J. J., Rothschild, B. J. (Eds.), The Sea, Wiley, New York, Vol. 12, 297-335.

983 de Boyer Montégut, C., Madec, G., Fischer, A. S., Lazar, A., Iudicone, D. 2004. Mixed layer
984 depth over the global ocean: An examination of profile data and a profile based climatology.
985 Journal of Geophysical Research, 109, C12003. http://dx.doi.org/10.1029/2004JC002378.
986
987 Demarcq, H., Barlow, R., Hutchings L. 2007. Application of a chlorophyll index derived
988 from satellite data to investigate the variability of phytoplankton in the Benguela ecosystem.
989 African Journal of Marine Science, 29, 271-282. doi:10.2989/AJMS.2007.29.2.11.194.
990
991 Demarcq, H., Barlow, R. G., Shillington, F. A. 2003. Climatology and variability of sea
992 surface temperature and surface chlorophyll in the Benguela and Agulhas ecosystems as
993 observed by satellite imagery. African Journal of Marine Science, 25, 363-372.
994 doi:10.2989/18142320309504022.
995
996 Devred, E., Sathyendranath, S., Stuart, V., Platt, T. 2011. A three component classification of
997 phytoplankton absorption spectra: Applications of ocean-colour data. Remote Sensing of
998 Environment, 115, 2255-2266. http://dx.doi.org/10.1016/j.rse.2011.04.025.
999
1000 Doney, S. C., Ruckelshaus, M., Emmett Duffy, J., Barry, J. P., Chan, F., English, C. A.,
1001 Galindo, H. M., Grebmeier, J. M., Hollowed, A. B., Knowlton, N., Polovina, J., Rabalais, N.
1002 N., Sydeman, W. J., Talley, L. D. 2012. Climate change impacts on marine ecosystems.
1003 Annual Review of Marine Science, 4, 11-37, doi: 10.1146/annurev-marine-041911-111611.
1004
1005 Durgadoo, J. V., Ansorge, I. J., Lutjeharms, J. R. E. 2010. Review: Oceanographic
1006 observations of eddies impacting the Prince Edward Islands, South Africa. Antarctic Science,
1007 22, 211-219. doi:10.1017/S0954102010000088.

Gibberd, M.-J., Kean, E., Barlow, R., Thomalla, S., Lucas, M. 2013. Phytoplankton chemotaxonomy in the Atlantic sector of the Southern Ocean during late summer 2009. Deep-Sea Research I, 78, 70-78. http://dx.doi.org/10.1016/j.dsr.2013.04.007.

Gregg, W. W., Casey, N. W. 2004. Global and regional evaluation of the SeaWiFS chlorophyll data set. Remote Sensing of Environment, 93, 463-479. doi:10.1016/j.rse.2003.12.012.

Gregg, W. W., Rousseaux, C. S. 2014. Decadal trends in global pelagic ocean chlorophyll: A new assessment integrating multiple satellites, in situ data, and models. Journal of Geophysical Research Oceans, 119, 5921-5933. doi:10.1002/2014JC010158.

Hirata, T., Hardman-Mountford, N. J., Barlow, R., Lamont, T., Brewin, R., Smyth, T., Aiken, J. 2009. An inherent optical property approach to the estimation of size-specific photosynthetic rates in eastern boundary upwelling zones from satellite ocean colour: An initial assessment. Progress in Oceanography, 83, 393-397. doi:10.1016/j.pocean.2009.07.019.

Hofmann, G. E., Todgham, A. E. 2010. Living in the now: physiological mechanisms to tolerate a rapidly changing environment. Annual Review of Physiology, 72, 127-145, doi: 10.1146/annurev-physiol-021909-135900.

Hutchings, L.,van der Lingen, C. D., Shannon, L. J., Crawford, R. J. M., Verheye, H. M. S., Bartholomae, C. H., van der Plas, A. K., Louw, D., Kreiner, A., Ostrowski, M., Fidel, Q.,

Barlow, R. G., Lamont, T., Coetzee, J., Shillington, F., Veitch, J., Currie, J. C., Monteiro, P. M. S. 2009. The Benguela Current: an ecosystem of four components. Progress in Oceanography, 83,15-32, doi:10.1016/j.pocean.2009.07.046.

IOCCG. 2014. Phytoplankton Functional Types from Space. S. Sathyendranath (Ed.), Reports of the International Ocean-Colour Coordinating Group, No. 15, Dartmouth, Canada.

Kahru, M., Mitchell, B. G. 2010. Blending of ocean colour algorithms applied to the Southern Ocean. Remote Sensing Letters, 1, 119-124. doi:10.1080/01431160903547940.

Kirkman, S. P., Blamey, L., Lamont, T., Field, J. F., Bianchi, G., Huggett, J. A., Hutchings, L., Jackson-Veitch, J., Jarre, A., Lett, C., Lipiński, M. R., Mafwila, S. W., Pfaff, M. C., Samaai, T., Shannon, L. J., Shin, Y-J., van der Lingen, C. D., Yemane, D. 2016. Spatial characterisation of the Benguela ecosystem for ecosystem-based management. African Journal of Marine Science, 38, 7-22. doi: 10.2989/1814232X.2015.1125390.

Kyewalyanga, M. S., Naik, R., Hedge, S., Raman, M., Barlow, R., Roberts, M. 2007. Phytoplankton biomass and primary production in the Delagoa Bight, Mozambique: application of remote sensing. Estuarine, Coastal and Shelf Science, 74, 429-436. doi:10.1016/j.ecss.2007.04.027.

Lamont, T., Barlow, R. G. 2015. Environmental influence on phytoplankton production during summer on the KwaZulu-Natal shelf of the Agulhas ecosystem. African Journal of Marine Science, 37, 485-501. doi: 10.2989/1814232X.2015.1108228.

Lamont, T., Barlow, R. G., Kyewalyanga, M. S. 2014a. Physical drivers of phytoplankton production in the southern Benguela upwelling system. Deep-Sea Research I, 90, 1-16. http://dx.doi.org/10.1016/j.dsr.2014.03.003.

Lamont, T., Barlow, R. G., Morris, T., van den Berg, M. A. 2014b. Characterisation of mesoscale features and phytoplankton variability in the Mozambique Channel. Deep-Sea Research II, 100, 94-105. doi: http://dx.doi.org/10.1016/j.dsr2.2013.10.019.

Lamont, T., Roberts, M. J., Barlow, R. G., Morris, T., van den Berg, M. A. 2010. Circulation patterns in the Delagoa Bight, Mozambique, and the influence of deep ocean eddies. African Journal of Marine Science, 32, 553-562. doi:10.2989/1814232X.2010.538147.

Lamont, T., van den Berg, M. A., Barlow, R. G. 2016. Agulhas Current influence on the shelf dynamics of the KwaZulu-Natal Bight. Journal of Physical Oceanography, 46, 1323-1338. doi: http://dx.doi.org/10.1175/JPO-D-15-0152.1.

Laubscher, R. K., Perissinotto, R., McQuaid, C. D. 1993. Phytoplankton production and biomass at frontal zones in the Atlantic sector of the Southern Ocean. Polar Biology, 13, 471-481. doi:10.1007/BF00233138.

Leal., M. C., Sá, C., Nordez, S., Brotas, V., Paula, J. 2009. Distribution and vertical dynamics of planktonic communities at Sofala Bank, Mozambique. Estuarine, Coastal and Shelf Science, 84, 605-616, doi: 10.1016/j.ecss.2009.07.028.

Lévy, M., Shankar, D., André, J.-M., Shenoi, S. S. C., Durand, F., de Boyer Montégut, C. 2007. Basin-wide seasonal evolution of the Indian Ocean's phytoplankton blooms. Journal of Geophysical Research, 112, C12014, http://dx.doi.org/10.1029/2007JC004090.

Lin, J., Cao., W., Wang, G., Hu, S. 2014. Satellite-observed variability of phytoplankton size classes associated with a cold eddy in the South China Sea. Marine Pollution Bulletin, 83, 190-197. http://dx.doi.org/10.1016/j.marpolbul.2014.03.052.

Louw, D. C., van der Plas, A. K., Mohrholz, V., Wasmund, N., Junker, T., Eggert, A. 2016. Seasonal and interannual phytoplankton dynamics and forcing mechanisms in the northern Benguela upwelling system. Journal of Marine Systems, 157, 124-134. http://dx.doi.org/10.1016/j.jmarsys.2016.01.009.

Lutjeharms, J. R. E. 2006. The Agulhas Current. Springer, 329 pp.

Lutjeharms, J. R. E., Valentine, H. R. 1984. Southern Ocean thermal fronts south of Africa. Deep-Sea Research I, 31, 1461-1475. doi:10.1016/0198-0149(84)90082-7.

Lutjeharms, J. R. E., Valentine, H. R., van Ballegooyen, R. C. 2000. The hydrography and water masses of the Natal Bight, South Africa. Continental Shelf Research, 20, 1907-1939. doi:10.1016/S0278-4343(00)00053-4.

Lutjeharms, J. R. E., Walters, N. M., Allanson, B. R. 1985. Oceanic frontal systems and biological enhancement. In: Antarctic nutrient cycles and food webs. Siegfried W. R. Condy, P., Laws, R. M. (Eds.), Springer-Verlag, Berlin, 11-21.

Marañón, E., Holligan, P. M., Barciela, R., González, N., Mouriño, B., Pazó, M. J., Varela, M. 2001. Patterns of phytoplankton size structure and productivity in contrasting open-ocean environments. Marine Ecology Progress Series, 216, 43-56.

McQuaid, C. D., Froneman, P. W. 2008. Biology in the oceanographic environment. In: S. L. Chown, P. W. Froneman (Eds.) The Prince Edward Islands: Land-Sea interactions in a changing ecosystem, Sun Press, Stellenbosch, 97-120.

Moore, J. K., Abbott, M. R. 2002. Surface chlorophyll concentrations in relation to the Antarctic Polar Front: seasonal and spatial patterns from satellite observations. Journal of Marine Systems, 37, 69-86.

Mordasova, N. V. 1980. Chlorophyll in the southwestern Indian Ocean in relation to hydrologic conditions. Oceanology, 20, 75-79.

Moré, J. J. 1978. The Levenberg-Marquardt algorithm: implementation and theory. In: Numerical Analysis, Watson, G. A. (Ed.), Springer-Verlag, Berlin, 105-116.

O'Connor, M. I., Piehler, M. F., Leech, D., Anton, A., Bruno, J. F. 2009. Warming and resource availability shift food web structure and metabolism. PLoS Biology, 7 (8), e1000178. doi:10.1371/journal.pbio.1000178.

1130 Perissinotto, R. Duncombe Rae, C., Boden, B. P., Allanson, B. R. 1990. Vertical stability as a
1131 controlling factor of the marine phytoplankton production at the Prince Edward Island
1132 Archipelago (Southern Ocean). Marine Ecology Progress Series, 60, 205-209
1133
1134 Pitcher, G. C., Brown, P. C., Mitchell-Innes, B. A. 1992. Spatio-temporal variability of
1135 phytoplankton in the southern Benguela upwelling system. South African Journal of Marine
1136 Science 12, 439-456. doi:10.2989/02577619209504717.
1137
1138 Pitcher, G. C., Nelson, G. 2006. Characteristics of the surface boundary layer important to the
1139 development of red tide on the southern Namaqua shelf of the Benguela upwelling system.
1140 Limnology and Oceanography, 51, 2660-2674. doi: 10.4319/lo.2006.51.6.2660.
1141
1142 Platt, T., Sathyendranath, S. 2008. Ecological indicators for the pelagic zone of the ocean
1143 from remote sensing. Remote Sensing of Environment, 112, 3426-3436. doi:
1144 10.1016/j.rse.2007.10.016.
1145
1146 Platt, T., Subba Rao, D. W., Irwin, B. 1983. Photosynthesis of picoplankton in the
1147 oligotrophic ocean. Nature, 301, 702-704. doi:10.1038/301702a0.
1148
1149 Pripp, T., Gammelsrød T., Krakstad, J. O. 2014. Physical influence on biological production
1150 along the western shelf of Madagascar. Deep-Sea Research II, 100, 174-183.
1151 http://dx.doi.org/10.1016/j.dsr2.2013.10.025.
1152

1153 Probyn, T. A. 1992. The inorganic nitrogen nutrition of phytoplankton in the southern
1154 Benguela: new production, phytoplankton size and implications for pelagic foodwebs. South
1155 African Journal of Marine Science, 12, 411-420.
1156
1157 Quartly, G., Srokosz, M. 2004. Eddies in the southern Mozambique Channel. Deep-Sea
1158 Research II, 51, 69-83. doi:10.1016/j.dsr2.2003.03.001.
1159
1160 Ridderinkhof, H., de Ruijter, W. P. M. 2003. Moored current observations in the
1161 Mozambique Channel. Deep-Sea Research II, 50, 1933-1955. doi:10.1016/S0967-
1162 0645(03)00041-9.
1163
1164 Roberts, M. J., van der Lingen, C. D., Whittle, C., van den Berg, M. 2010. Shelf currents, lee-
1165 trapped and transient eddies on the inshore boundary of the Agulhas Current, South Africa:
1166 Their relevance to the KwaZulu-Natal sardine run. African Journal of Marine Science, 32,
1167 423-447. doi:10.2989/1814232X.2010.512655.
1168
1169 Sá, C., Leal, M. C., Silva, A., Nordez, S., André, E., Paula, J., Brotas, V. 2013. Variation in
1170 phytoplankton assemblages along the Mozambique coast as revealed by HPLC and
1171 microscopy. Journal of Sea Research, 79, 1-11.
1172 http://dx.doi.org/10.1016/j.seares.2013.01.001.
1173
1174 Sammartino, M., Di Cicco, A., Marullo, S., Santoleri, R. 2015. Spatio-temporal variability of
1175 micro-, nano-, and picophytoplankton in the Mediterranean Sea from satellite ocean colour
1176 data of SeaWiFS, Ocean Science, 11, 759-778. doi:10.5194/os-11-759-2015.
1177

Sarmiento, J. L., Gruber, N., Brzezinski, M. A., Dunne, J. P. 2004. High-latitude controls of thermocline nutrients and low latitude biological productivity. Nature, 427, 56-60, doi: 10.1038/nature02127.

Sathyendranath, S., Stuart, V., Cota, G., Maas, H., Platt, T. 2001. Remote sensing of phytoplankton pigments: a comparison of empirical and theoretical approaches. International Journal of Remote Sensing, 22, 249-273. doi:10.1080/014311601449925.

Schlitzer, R. 2002. Carbon export fluxes in the Southern Ocean: results from inverse modelling and comparison with satellite-based estimates. Deep-Sea Research II, 49, 1623-1644, doi: 10.1016/S0967-0645(02)00004-8

Schouten, M. W., de Ruijter, W. P. M., Ridderinkhof, H. 2005. A seasonal intrusion of subtropical water in the Mozambique Channel. Geophysical Research Letters, 32, L18601, doi:10.1029/2005GL023131.

Schouten, M. W., de Ruijter, W. P. M., van Leeuwen, P. J., Ridderinkhof, H. 2003. Eddies and variability in the Mozambique Channel. Deep-Sea Research II, 50, 1987-2003. doi:10.1016/S0967-0645(03)00042-0.

Shannon, L. V., Pillar, S. C. 1986. The Benguela ecosystem. Part III. Plankton. Oceanography and Marine Biology: An Annual Review, 24, 65-170.

Swart, S., Thomalla, S. J., Monteiro, P. M. S. 2015. The seasonal cycle of mixed layer dynamics and phytoplankton biomass in the Sub-Antarctic Zone: A high-resolution glider

experiment. Journal of Marine Systems, 147, 103-115. http://dx.doi.org/10.1016/j.jmarsys.2014.06.002.

Tew Kai, E., Marsac. F. 2009. Patterns of variability of sea surface chlorophyll in the Mozambique Channel: a quantitative approach. Journal of Marine Systems, 77, 77-88. doi:10.1016/j.jmarsys.2008.11.007.

Thomalla, S. J., Fauchereau, N, Swart, S., Monteiro, P. M. S. 2011a. Regional scale characteristics of the seasonal cycle of chlorophyll in the Southern Ocean. Biogeosciences, 8, 2849-2866. doi:10.5194/bg-8-2849-2011.

Thomalla, S. J., Waldron, H. N., Lucas, M. I., Read, J. F., Ansorge, I. J., Pakhomov, E. 2011b. Phytoplankton distribution and nitrogen dynamics in the southwest indian subtropical gyre and Southern Ocean waters. Ocean Science, 7, 113-127. doi:10.5194/os-7-113-2011.

Tremblay, J.-E., Legendre, L. 1994. A model for the size-fractionated biomass and production of marine phytoplankton. Limnology and Oceanography, 39, 2004-2014.

Tsugawa, M., Hasumi, H. 2010. Generation and growth mechanism of the Natal pulse. Journal of Physical Oceanography, 40, 1597-1616. doi:10.1175/2010JPO4347.1.

Uitz, J., Claustre, H., Morel, A., Hooker, S. B. 2006. Vertical distribution of phytoplankton communities in the open ocean: An assessment based on surface chlorophyll. Journal of Geophysical Research, 111, C08005. http://dx.doi.org/10.1029/2005JC003207.

1228 Veitch, J., Penven, P., Shillington, F. 2009. The Benguela: A laboratory for comparative
1229 modelling studies. Progress in Oceanography, 83, 296-302.
1230 doi:10.1016/j.pocean.2009.07.008.
1231
1232 Verheye, H. M., Lamont, T., Huggett, J. A., Kreiner, A., Hampton, I. 2016. Plankton
1233 productivity of the Benguela Current Large Marine Ecosystem (BCLME). Environmental
1234 Development, 17, 75-92. http://dx.doi.org/10.1016/j.envdev.2015.07.011.
1235
1236 Ward, B. A. 2015. Temperature-correlated changes in phytoplankton community structure are
1237 restricted to polar waters. PLoS ONE, 10(8), e0135581.
1238 http://dx.doi.org/10.1371/journal.pone.0135581.
1239
1240 Werdell, P. J., Bailey, S. W. 2005. An improved in-situ bio-optical data set for ocean colour
1241 algorithm development and satellite data production validation. Remote Sensing of
1242 Environment, 98, 122-140. http://dx.doi.org/10.1016/j.rse.2005.07.001.
1243
1244 Weeks, S. J., Barlow, R., Roy, C., Shillington, F. A. 2006. Remotely sensed variability of
1245 temperature and chlorophyll in the southern Benguela: upwelling frequency and
1246 phytoplankton response. African Journal of Marine Science, 28, 493-509.
1247 doi:10.2989/18142320609504201.
1248
1249 Zubkov, M. V., Quartly, G. D. 2003. Ultraplankton distribution in surface waters of the
1250 Mozambique Channel – flow cytometry and satellite imagery. Aquatic Microbial Ecology,
1251 33, 155-161.